Doctoral Dissertation

A Study of High-Precision Array Antenna System for Adaptive Antenna in Mobile Communication

(移動体通信におけるアダプティブアンテナのためのアレーアンテナシステム高精度化の研究)

December 17, 2004

Under the Supervision of

Professor Hiroyuki Arai

Presented by

Yuki Inoue

Graduate School of Engineering

Yokohama National University, Japan

Abstract

The construction of a low-cost and reliable array antenna system is required to facilitate the practical use of the adaptive antenna in the mobile communication field. The array antenna system can be verified by DOA (Direction of Arrival) estimation. This dissertation describes the attempt to achieve a high-precision adaptive antenna and the examination of this device, which suppresses the number of array elements, in a real mobile communication environment. In chapter 2, we evaluate the array antenna system by DOA estimation, and on the basis of this evaluation, we clarify the problems related to the hardware and propagation environment of the array antenna system. It is necessary to model the array antenna system both statistically and quantitatively based on measurements. First, we formulate the array antenna and DOA estimation and explain the prototype array antenna systems. The prototype system has been improved after every evaluation. Next, an evaluation method using a rotating array antenna is proposed. Using a rotating array antenna and DOA estimation, this method can be used to evaluate the array antenna system in detail. Further, we analyze the error factor on the basis of an experiment in the anechoic chamber. In chapter 3, we undertake a detailed examination of the errors resulting from inaccuracies in array element positions, mutual coupling of elements, and plane-wave approximation in which the distance between transmitting and receiving antennas is small. Element position and mutual coupling influence each other and affect the antenna element pattern. First, we formulate the array antenna that takes into account the effects of the antenna element pattern and use the moment method to quantitatively and statistically, analyze the mutual coupling and DOA estimation error. The DOA estimation error is dependent on null steering of the adaptive antenna. Next, changing simulation is performed by varying the extent of

mutual coupling. It is impossible to realize an antenna without coupling; however, the coupling can be suppressed. This property will be useful in manufacturing the antenna array. In chapter 4, we propose a calibration method for suppressing the error factors. Steering vector compensation method is the most basic calibration method. Coupling calibration using a fixed calibration antenna can eliminate these problems and it can be calibrated during operation. The correlation matrix estimation method for the transmission array antenna is demonstrated experimentally in the anechoic chamber. Additionally, based on the discussion in chapter 3, the time of calibration of the pattern is reduced by employing the element interval tuning method and a low-coupling array antenna system. The array antenna element pattern is changed due to several error factors; however, optimum adjustment of the element interval, mutual coupling, and number of elements results in a high-precision array antenna system with reduced errors. In conclusion, inaccuracy of array element position and mutual coupling of elements influence each other and cause a DOA estimation error or adaptive null steering in the antenna element pattern. A high-precision array antenna system can be achieved through optimal adjustment of these factors.

Contents

Chapter 1

Introduction

1.1 Introduction

In recent years, there has been a remarkable progress in mobile communication. High-speed, large data transmission services, such as internet access via a mobile terminal and video conferencing with mobile phones, are gaining popularity. Therefore, ensuring sufficient channel capacity is one of the most important factors in mobile communication. Sector antennas and micro cells or pico cells, which are smaller than usual cells, have thus far been introduced in high-traffic areas [1]. However, these cells will have limitations concerning increase in the number of base stations. The adaptive antenna [2] is an antenna that responds to the environment and changes its pattern adaptively using an array antenna, and it is capable of suppressing interference. Since 1990, the application of adaptive antennas to mobile communication has been extensively studied. Suppressing interference could effectively ensure sufficient channel capacity. Adaptive antenna theory has now been defined, and research in this field has produced similar results. However, adaptive antennas have rarely been put to practical use due to factors such as cost.

1.2 Array Antenna System Technology

An antenna with two or more antenna elements that are arranged and excited is termed an array antenna. The array antenna, receiver, and the signal processing division collectively constitute the array antenna system. The array antenna system is used for adaptive antenna and DOA (direction of arrival) estimation.

1.2.1 Adaptive Antenna

The adaptive antenna is an array antenna that performs an adaptive control of the pattern in order to maximize the SINR (Signal to Interference and Noise Ratio) [3]. The adaptive antenna is occasionally distinguished from the multibeam antenna, which exhibits two or more patterns, and the smart antenna that consists of both the adaptive and multibeam antennas [4]. However, in this paper, the term “adaptive antenna” is used synonymously with “smart antenna.” Since the 1950s, the adaptive antenna has been evaluated as technology that can eliminate military radar jamming and various algorithms with subsequent enhancements have been proposed [2]. However, due to its large size and high cost of production, the device was initially used only for military purposes. The achievement of a small, low-priced system by the advancement of the LSI technology is in prospect and the application of the adaptive antenna in mobile communication has been studied intensively since around 1990 [5][6]. The theory has now been defined and the research marshaled. With the exception of its introduction in 1998 in Japan as a part of the base station of PHS (Personal Handyphone System), the adaptive antenna has rarely been used in practical applications due to factors such as its high cost of production [7].

The model of an adaptive antenna is shown in Figure 1.1. The pattern is controlled by dynamically varying the phase and amplitude of the received signal of

each element. The adaptive antenna performs two functions: it directs beams toward the desired signals and nulls toward the undesired signals. The adaptive algorithms are capable of directing the nulls [2], and they differ from the phased-array antenna algorithms that direct only the beam toward the desired signal. It is necessary to distinguish the desired and undesired signals in an adaptive antenna that displays automatic control. Figure 1.2 shows the examples of adaptive antenna patterns. Figure 1.2 (a) depicts a beam and null that are directed toward the desired and undesired signals, respectively, and Figure 1.2 (b) shows a null that is directed toward the desired signals. Correct control of beams and nulls is indispensable for the adaptive antenna.

The weight control algorithm of the adaptive antenna can be classified into the MMSE (Minimum Mean Square Error) method [3][8], the CMA (Constant Modulus Algorithm) method [9], the MSN (Maximum Signal to Noise Ratio) method [10], the DCMP (Directionally Constrained Minimization of Power) method [11], the ZF (Zero Forcing) method, and the PI (Power Inversion) method [12].

1.2.2 DOA Estimation

Beamformer method is the most basic method employed in DOA estimation with an array antenna, wherein the main beam scans and determines the direction in which the output power of the array becomes maximum [2]. When this method is devised by the filter theory of the signal processing field, it agrees with a spatial Fourier transform method. This implies that DOA can be estimated according to the direction of maximum output power by performing fast Fourier transform on the output of the receiver array. In order to increase the number of outputs in this direction, 0 series must be added after the array output before performing the Fourier transform. However, the amount of information concerning direction remains unchanged even after increasing the number of outputs because the resolution is limited by the array arrangement, that is, the main beam width of the array antenna or the sampling number and interval in the

filter theory.

The resolution can be improved by using the null instead of the beam in DOA estimation. The LP (Liner Prediction) method is a basic method of null steering. The principle of scanning nulls in the LP method corresponds to minimizing the output power of the array antenna in the PI and DCMP methods of the adaptive antenna. A reciprocal spectrum of the LP method is identical to a pattern of the PI and DCMP methods. MUSIC (Multiple Signal Classification) [13] and ESPRIT (Estimation of Signal Parameters via Rotation Invariance Techniques) [14] algorithms are improved versions of the LP method that are capable of achieving high-resolution DOA estimation. An example of DOA estimation by these algorithms is shown in Figure 1.3 and their characteristics are listed in Table 1.2.

DOA estimation has developed separately from the adaptive antenna. However, several algorithms are based on the same principle. By comparing Figure 1.2 (b) with Figure 1.3, it is evident that null control of the adaptive antenna agrees with the DOA estimation. Since the pattern can be scanned electrically, the array antenna is widely used for DOA estimation. DOA estimation has several applications such as in beam control of adaptive antenna, measurement of propagation environment, radar technology, etc. In particular, in the field of mobile communication, a high-resolution measurement technology of propagation environment, such as power, direction, or delay characteristics in various environments, is required. It is possible to control the pattern based on factors such as the position of the terminal.

1.2.3 Adaptive Antenna and DOA Estimation

By restricting the evaluation to a null- and beam-pattern controlling adaptive antenna, the DOA estimation agrees with null control of the adaptive antenna. Hence, it can be said that a DOA estimation without system errors ensures null control of the

adaptive antenna without system errors. The converse is also true. Therefore, the performance of the array antenna system can be evaluated by the DOA estimation error.

On the other hand, there exist adaptive antennas that do not employ pattern controlling but maximize the SINR, as in the MMSE method. Such adaptive antennas can be controlled by including system errors and are convenient for a receiving system. However, such adaptive antennas cannot estimate performance on the basis of the pattern; hence, it is not necessary to suppress the DOA estimation error. Yet, even in the case of such algorithms, a DOA estimation without system errors results in an adaptive antenna without system errors.

1.3 Adaptive Antenna Implementation in Mobile Communication

1.3.1 Adaptive Antenna and Mobile Communication

The data transmission system in mobile communication has evolved with the use of the FDMA (Frequency Division Multiple Access), TDMA (Time Division Multiple Access), and CDMA (Code Division Multiple Access) methods; the CDMA method is currently the most commonly used method. In a CDMA system, the desired and undesired signals cannot be distinguished by considering the analog characteristics of the signal alone; this makes the application of the adaptive antenna in mobile communication systems difficult.

Table 1.1 shows a comparison of the typical adaptive antenna algorithms, which are being considered for application to mobile communication systems. The

information required to distinguish desired and undesired signals is prepared on the basis of a reference signal, which is a replica of the desired signal in the MMSE method, the DOA of the desired wave in MSN or DCMP method, and the array steering vector of the desired wave in ZF or regularization method. In the CMA method, the prepared information is not necessary if the desired signal possesses a constant envelope; however, it is essential undesired signals don't possesses a constant envelope. Irrespective of the algorithm used, it is necessary to distinguish between the desired and undesired signals by adding the preamble before the data symbol in a CDMA system.

1.3.2 Problems Concerning the Implementation of the Adaptive Antenna in Mobile Communication

The construction of a low-cost and reliable array antenna system is required to facilitate the practical use of the adaptive antenna in the mobile communication field. The cost of an array antenna system is most influenced by the number of antenna elements, that is, the number of channels, because it corresponds to the number of devices. However, a reduction of antenna elements reduces the number of treatable waves and leads to a decline in the performance of the adaptive antenna. This is because the general adaptive algorithm cannot process undesired waves greater than the number of array elements since, in array antenna theory, the number of elements corresponds to the number of nulls of the pattern.

On the other hand, the reliability of an array antenna system is dependent on the production accuracy of the array antenna or the calibration accuracy of a system. Calibration is usually performed in an anechoic chamber before operation; however, incorrect calibration of the system in the operating environment results in erroneous pattern control. This poses a major problem since it is very difficult to confirm the accuracy of the system during operation, particularly during transmission.

1.3.3 Evaluation and Calibration of the Array Antenna System

In most researches on adaptive antennas, propagation path and array antenna system are modeled and algorithms are compared by numerical calculations. Several measurements and evaluations are performed to obtain the propagation model in mobile communication, and the adaptive antenna is verified on the basis of this model. On the other hand, array antenna systems are often easily modeled without any measurements and the effects of difference in characteristics, mutual coupling, manufacturing error, etc., are rarely discussed. This is because evaluation is very difficult since the characteristics of the array antenna system vary according to composition or the device used. For example, in the modeling of mutual coupling between antenna elements, a single mode operation of the antenna and a linear coupling matrix are generally assumed [15]. However, the results of actual measurements cannot be explained by the single mode operation model alone since the mutual coupling changes due to the manufacturing error of the array antenna. Therefore, it is necessary to statistically and quantitatively model the array antenna system based on measurements.

DOA estimation can be used to verify the array antenna system. Studies evaluating the influence of mutual coupling and manufacturing error on DOA estimation have thus far been similar. For example, one study evaluates the influence of the difference in spacing between elements of a linear array antenna by simulation using DOA estimation [16], while another evaluates the influence of phase error and mutual coupling [17]. The former examines the error in element interval with respect to one-dimensional normal distribution errors, but it does not examine two-dimensional errors. The latter examines the error in the difference in spacing between the elements though phase error is examined in a single element. Moreover, in both studies, DOA remains unchanged, and it is necessary to discuss the error on the basis of the direction.

The calibration of the array antenna system is related to modeling. In mobile

communication, a system that can be calibrated during operation is key to the application of the adaptive antenna based on the modeling of array antenna systems [18]. For such systems, the methods for calibrating the device, or including the antenna, etc., are proposed; however, a mutual coupling calibration system is necessary when the antenna elements are few in number.

1.4 Conclusion

This chapter provided an outline of the adaptive antenna and DOA estimation with the array antenna system. The construction of a low-cost and reliable array antenna system is required to facilitate the practical use of the adaptive antenna in the mobile communication field. If DOA estimation has no system error, the adaptive antenna should also have no system error. Therefore, DOA estimation can be used to verify the array antenna system. In addition, the current situation and the problems in present research were presented with regard to evaluation and calibration of the array antenna system.

This paper describes the attempt to achieve a high-precision adaptive antenna and the examination of this device, which suppresses the number of array elements, in a real mobile communication environment. Using array antenna prototypes, we showed the influence of antenna characteristics, such as mutual coupling, manufacturing error, or the pattern for DOA estimation, both statistically and quantitatively. In addition, we propose a highly accurate adaptive antenna system by calibration.

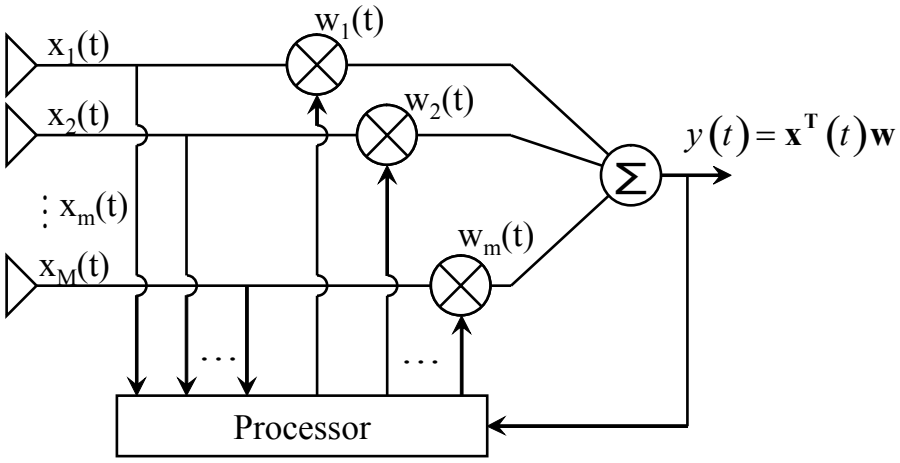

Figure 1.1: Adaptive antenna.

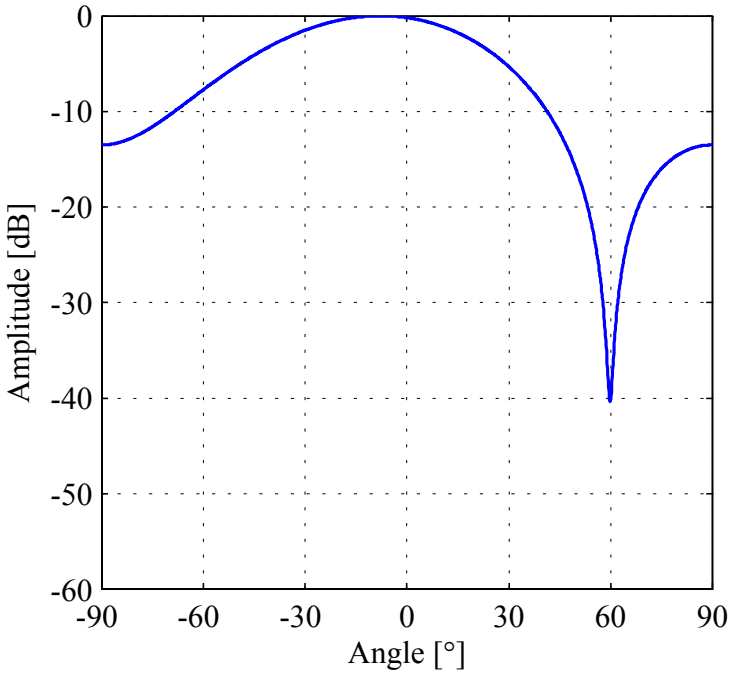

(a) 2-element array

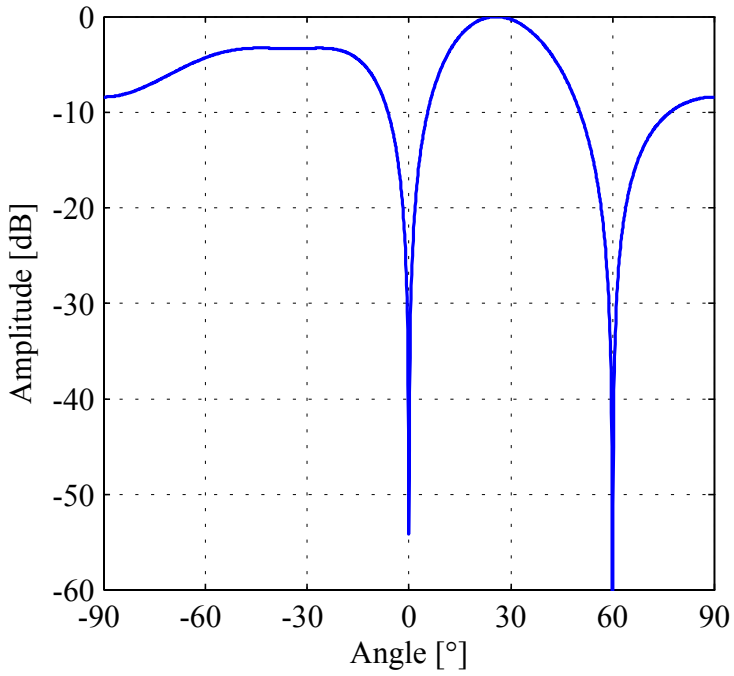

(b) 4-element array

Figure 1.2: Example of an adaptive antenna pattern (PI method).

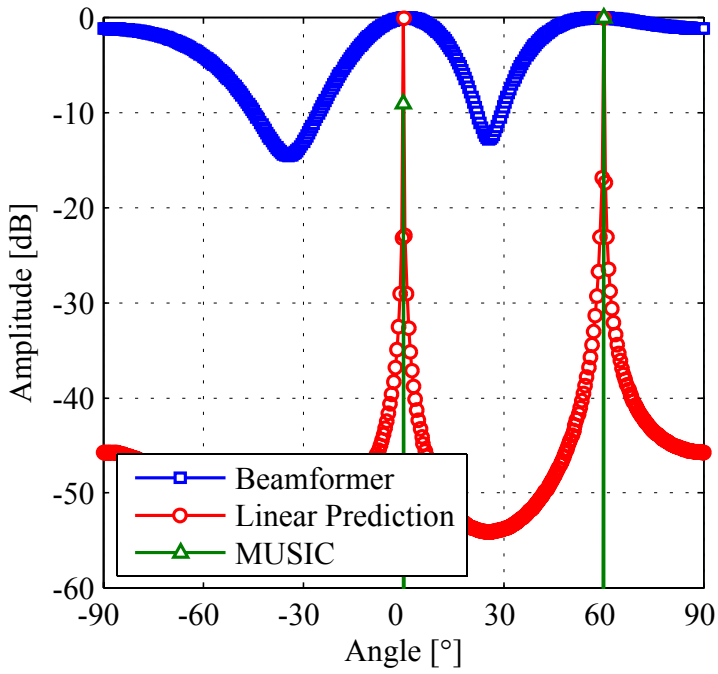

Figure 1.3: Example of DOA estimation.

Table 1.1: Comparison of the algorithms of the adaptive antenna.

Algorithm	Method to distinguish the desired signal	Operating condition	Operation in correlation interference	Others
MMSE	Reference signal (Replica of desired signal)	None	Synthesized with desired signal (Reference signal correlation decreases)	Complete symbol synchronization of the received signal
CMA	None	Envelope of desired signal is constant	Synthesized with desired signal	Another method is required to extract the desired signal from an interfering signal
MSN	DOA of desired signal	None	Suppressed with desired signal (Spatial smoothing is necessary)	DOA estimation and another method are required to extract the desired signal
DCMP	DOA of desired signal	None	Suppressed with desired signal (Spatial smoothing is necessary)	DOA estimation and another method are required to extract the desired signal
ZF Regulariza tion	Array steering vector of desired signal	None	Synthesized with desired signal	Channel estimation function (or DOA in a few correlation interference conditions) is required

PI	None	Power of undesired signal > desired signal; undesired wave number = array degree of freedom –1	Suppressed with desired signal (Spatial smoothing is necessary)	Unsuitable for mobile communication from the viewpoint of power

Table 1.2: DOA estimation algorithm.

	Beam scanning	Null scanning	
Algorithm	Beamformer method, Capon method	Linear predictive method, Least norm solution method, MUSIC method	ESPRIT method
Array antenna condition	The direction vector of the array is already known.		Two sub-arrays are identical and the direction vector between them is already known.

Table 1.3 Difference of time and spatial domain processing.

	Number of sampling devices	Delay signal of one or less than one symbol (Correlation interference)	Delay signal greater than one symbol (Decorrelation interference)
Time domain	One	Processing is easy	Removed with an interference canceller
Spatial domain	Number of sampling devices	It is necessary to suppress the correlation of the interference wave. (It is necessary to increase the number of sampling devices)	Removed

Chapter 2

Evaluation of the Array Antenna System by DOA Estimation

2.1 Introduction

In this chapter, we evaluate the array antenna system by DOA estimation, and on the basis of this evaluation, we clarify problems related to the hardware and propagation environment of the array antenna system. Array antenna systems are often modeled without any measurements and the effects of difference in characteristics, mutual coupling, manufacturing errors, etc., are rarely studied. The theory and measurements vary, particularly when the elements are few in number. It is necessary to model the array antenna system both statistically and quantitatively based on measurements. First, we formulate the array antenna by DOA estimation and explain the prototype array antenna systems. The prototype system has been improved after every evaluation. Next, an evaluation method using a rotating array antenna is proposed. This method can be used to evaluate the array antenna system in detail using a rotating array antenna and DOA estimation. Further, we analyze the error factor experimentally in an anechoic chamber.

2.2 Formulation

2.2.1 Formulation of the Array Antenna

First, we formulate a uniformly spaced linear array antenna ignoring mutual coupling between array elements and assume that the element patterns of the array antenna are identical. We consider narrow band plane waves W, where the center wavelength is λ, and the observed linear array antenna consists of d intervals with M antenna elements. Figure 2.1 shows the array antenna geometry. The output signal of the mth element can be described as follows:

$$x_m(t) = \sum_{w=1}^{W} s_w(t) \cdot a_m(\theta_w) + n_m(t) \tag{2.1}$$

$$\begin{aligned} \mathrm{a}_m(\theta_w) &= \exp\left[j2\pi \frac{f}{c} d(m-1)\sin\theta_w \right] \\ &= \exp\left[j\frac{2\pi}{\lambda} d(m-1)\sin\theta_w \right] \\ m &= 1,\cdots,M \end{aligned} \tag{2.2}$$

where s_w(t) and θ_w are the complex amplitude and DOA of the wth source, respectively (the vertical direction in terms of the array is assumed to be 0°), n_m(t) is the normally distributed noise with mean 0 and variance σ^2, f is the carrier frequency, and c is the luminous flux. Equation (2.1) can be expressed using vector representation as follows:

$$\mathbf{x}(t) = \mathbf{A}\mathbf{s}(t) + \mathbf{n}(t) \tag{2.3}$$

$$\mathbf{x}(t) = \begin{bmatrix} x_1(t) & x_2(t) & \cdots & x_M(t) \end{bmatrix}^T \tag{2.4}$$

$$\mathbf{A} = \begin{bmatrix} \mathbf{a}(\theta_1) & \mathbf{a}(\theta_2) & \cdots & \mathbf{a}(\theta_W) \end{bmatrix} \tag{2.5}$$

$$\begin{aligned} \mathbf{a}(\theta_w) = \Bigg[& 1 \quad \exp\left(j\frac{2\pi}{\lambda} d \sin\theta_w \right) \\ & \cdots \quad \exp\left(j(M-1)\frac{2\pi}{\lambda} d \sin\theta_w \right) \Bigg]^T \end{aligned} \tag{2.6}$$

$$\mathbf{s}(t) = \begin{bmatrix} s_1(t) & s_2(t) & \cdots & s_W(t) \end{bmatrix}^T \tag{2.7}$$

$$\mathbf{n}(t) = \begin{bmatrix} n_1(t) & n_2(t) & \cdots & n_M(t) \end{bmatrix}^T \tag{2.8}$$

where the superscript T denotes the transpose of the vector or matrix. $\boldsymbol{a}(\theta_w)$ is termed the "steering vector," which represents the receiving characteristics of the array antenna for the direction of θ_w.

Then, the array correlation matrix is defined as follows:

$$\begin{aligned} \mathbf{R}_{xx} &= E\left[\mathbf{x}(t)\mathbf{x}^H(t) \right] \\ &= \mathbf{ASA}^H + \sigma^2\mathbf{I} \end{aligned} \tag{2.9}$$

where $E[\cdot]$ denotes the expectation operator, the superscript H denotes the complex conjugate transpose of the vector or matrix, and $\boldsymbol{S}$ is the source correlation matrix defined as

$$\mathbf{S} = E\left[\mathbf{s}(t)\mathbf{s}^H(t)\right] \tag{2.10}$$

The eigenvalues and associated eigenvectors of $\boldsymbol{R_{xx}}$ are defined as λ_m and $\boldsymbol{e_m}$, respectively; therefore, the correlation matrix takes the following form:

$$\begin{aligned}\mathbf{R}_{xx} &= \sum_{m=1}^{M} \lambda_m \mathbf{e}_m \mathbf{e}_m{}^H \\ &= \mathbf{E}\boldsymbol{\Lambda}\mathbf{E}^H\end{aligned} \tag{2.11}$$

where $\boldsymbol{E}$ is a row matrix of $\boldsymbol{e_m}$ and $\boldsymbol{\Lambda}$ is a diagonal matrix of λ_m.

When correlation between sources and noise has no correlation with source, the eigenvalues of $\boldsymbol{R_{xx}}$ are related as follows:

$$\lambda_1 \geq \lambda_2 \geq \cdots \geq \lambda_W > \lambda_{W+1} = \cdots = \lambda_M = \sigma^2 \tag{2.12}$$

This implies that an eigenvalue can be divided into a signal component and a noise component; defined as $\boldsymbol{\Lambda_S}$ and $\boldsymbol{\Lambda_N}$, respectively, and the corresponding eigenvectors are defined as $\boldsymbol{E_S}$ and $\boldsymbol{E_N}$, respectively. Thus, equation (2.12) can be expressed as

$$\mathbf{R}_{xx} = \mathbf{E}_S \boldsymbol{\Lambda}_S \mathbf{E}_S{}^H + \mathbf{E}_N \boldsymbol{\Lambda}_N \mathbf{E}_N{}^H \tag{2.13}$$

2.2.2 Formulation of DOA Estimation

As shown in section 1.2.2, the algorithm of DOA estimation using an array antenna is categorized based on the principle of beam and null steering. Both methods require the steering vector of the array antenna for estimation. However, in the ESPRIT

method, the steering vector of two identical sub-arrays is already known.

Here, we formulate a representation for the MUSIC method. On comparing equations (2.9) and (2.13), a component of $\boldsymbol{E}_N$ is perpendicular to the steering vector $\boldsymbol{A}$.

$$\begin{aligned} &\mathbf{e}_j{}^H \mathrm{a}(\theta_i) = 0 \\ &i = 1, \cdots, W \\ &j = W+1, \cdots, M \end{aligned} \tag{2.14}$$

On the basis of this relation, DOA estimation is conducted with the following equation:

$$\begin{aligned} \mathrm{P}_{MUSIC}(\theta) &= \frac{\mathrm{a}^H(\theta)\mathrm{a}(\theta)}{\sum_{j=W+1}^{M} \left| \mathbf{e}_j{}^H \mathrm{a}(\theta) \right|^2} \\ &= \frac{\mathrm{a}^H(\theta)\mathrm{a}(\theta)}{\mathrm{a}^H(\theta)\mathbf{E}_N\mathbf{E}_N{}^H \mathrm{a}(\theta)} \end{aligned} \tag{2.15}.$$

The denominator is a scalar product between the steering vector and the noise eigenvector; $P_{MUSIC}(\theta)$ becomes infinite when θ satisfies equation (2.14). The plot of $P_{MUSIC}(\theta)$ with varying values of θ is called the MUSIC spectrum and the peaks represent the estimated DOA.

Therefore, DOA estimation by the MUSIC method has the following requirements. First, correlation of arriving waves should be low and should be absent with noise. When the correlation is high, the SSP (Spatial Smoothing Preprocessing) method [19] is proposed in order to suppress the correlation. Second, the number of waves W should be smaller than the number of elements M. Third, accurate information regarding the steering vector $\boldsymbol{a}(\theta)$ and W should be previously available.

2.3 Evaluation of Prototype Array Antenna Systems

2.3.1 Evaluation Method of the Array Antenna System by Rotating the Receiving Antenna

In order to verify a system by DOA estimation, an array antenna verification system with DOA estimation is proposed. In this system, DOA is varied by rotating the receiving array antenna on a rotator with a fixed transmitting antenna, and the estimation error is verified. Since the transmitting antenna is fixed, a highly accurate verification is obtained.

Figure 2.7 shows the x-y coordinate system in which the center of rotation of the receiving array antenna lies at the origin, the angle of the receiving array antenna to the x axis is defined as ρ, and the direction of the transmitting antenna to the y axis is defined as τ_w. The current DOA θ_w at the receiving point is

$$\theta_{\mathrm{w}} = \tau_w - \rho \tag{2.16}.$$

For example, when the transmitting antenna is on the y axis ($\tau_w = 0$), $\theta_w = -\tau_w$. The DOA estimation error δ_w is defined as

$$\delta_w = \theta_{\mathrm{w}} - \varepsilon_{\mathrm{w}} \tag{2.17}$$

where ε_w is the estimated angle.

The DBF (Digital Beam Forming) receiver is composed of cables, frequency converters, filters, etc. These characteristics differ in each channel and vary depending

on time, temperature, etc. Thus, since the characteristics differ from channel to channel, it is necessary to calibrate the phase and amplitude in each channel. The phase and amplitude of the received signal in each channel of the DBF array antenna were adjusted by calibration before carrying out measurements when a sine wave was transmitted to the receiving array antenna ($\tau_w = \rho = 0$ in Figure 2.7). When the arriving wave is assumed to be a plane wave, the received signal in each element becomes equal. The dispersion of each antenna element, cables, and low-cost RF circuits can be restrained by this procedure.

2.3.2 Prototype Array Antenna Systems

The basic construction of an array antenna system is shown in Figure 2.2. The signal received from the array antenna is converted to low frequency in the DBF receiver and stored in the PC's (Personal computer) memory using an AD (Analog to Digital) converter. This operation is synchronously carried out for each channel. This array antenna system offers the best configuration for mobile communication since multiple patterns can be steered simultaneously. It is possible to operate all adaptive algorithms and all DOA estimation algorithm by using this system for measurement.

Thus far, we have designed some prototype array antenna systems in our laboratory and have subsequently tested and improved each one. Table 2.1 lists the characteristics of the prototype receivers. The block diagram of the initial model is shown in Figure 2.3. In this model, the RF signal received from the array antenna (sleeve antennas are arrayed in half-wavelength intervals) passes through three steps of frequency conversion and orthogonal decomposition, and we obtain the I (In phase) and Q (Quadrature phase) signals for each element as outputs. The phase and amplitude of each channel can be independently controlled within ±90° and ±5 dB, respectively, using the controller attached to the receiver. Before designing the receiver, the following points were noted:

1. The electrical length from RF input to IQ output is kept constant between channels.

2. The phase and amplitude of the LO input to the mixer are kept constant between channels.

3. The system should be designed such that the characteristics of the circuits (phase and gain) are not easily influenced by external factors. (The high-pass filter and low-pass filter are used instead of the band-pass filter)

4. Independent phase and amplitude adjustment circuits are installed in each channel.

However, this composition poses a problem—the phase and amplitude cannot be adjusted independently (amplitude changes when the phase is changed), the shift in the range of the phase is limited, and the orthogonality of IQ suffers due to the instability of an internal oscillator. These problems were solved by incorporating a series of improvements. The composition of the improved receiver is shown in Figure 2.4. The following adjustments were made:

1. The IF (Intermediate Frequency) signal was sampled with an AD converter before orthogonal decomposition and was detected with digital signal processing.

2. Phase adjustment circuit is installed in the LO section.

3. Remote phase and amplitude adjustment controllers are used.

4. A highly accurate external oscillator is used.

As a result, each channel outputs an IF signal that is detected by digital signal processing. A merit of this method is that it reduces the circuit scale although it requires a high-speed AD converter. In addition, by installing the phase adjustment

circuit in the LO section, independent adjustment of the phase and amplitude was achieved. Adjustment controllers were remotely installed in order to adjust the phase and amplitude. Moreover, instability of the transmitter has been reduced by using a highly accurate external oscillator for the LO.

In addition, with the use of a YIG (Yttrium Iron Garnet) tunable filter, carrier frequency could be varied and it corresponded with various experimental conditions. Due to its high cost, the YIG tunable filter is generally used in spectrum analyzers or military applications. However, this filter was adopted in this system because it offers the advantage of variable frequency range. The general view and a block diagram of the receiver are shown in Figure 2.5 and Figure 2.6, respectively. The prototype receiver obtains an IF output of 40 MHz corresponding to an input in the range of 2 ~ 8 GHz for every four channels. The phase adjustment of ±90° is possible for proofreading between channels and the amplitude can be adjusted within the range of 0 ~ 20 dB. The circuit is composed of a two-stage mixer and amplifiers and filters. The carrier frequency can be varied according to the input frequency of the LO and the voltage of the YIG tunable filter can be controlled.

2.3.3 Analysis of Error Factors

In this section, we analyse the model with a transmission source installed in front of the array, as shown in Figure 2.7, in order to examine the estimation error in detail and to specify the error factors. The 1st and 3rd DBF receivers (Table 2.1) are used for this examination at 2.6 GHz and 8.45 GHz, respectively. We use the MUSIC algorithm for DOA estimation inside the anechoic chamber. First, we calibrate the amplitude and phase of each element in the IF band using the adjustment circuit inside the receiver and a digital oscilloscope. The DOA is then estimated using the system. The received IF signals are sampled simultaneously by the AD converter and stored in the PC. The DOA is estimated by the MUSIC algorithm by off-line processing. The

estimation error is then measured. The relation between the DOA θ_w and estimation error δ_w is shown in Figure 2.8 wherein θ_w is varied at every degree. Figure 2.8 shows that the estimation error δ_w increases with the absolute value of DOA $|\theta_w|$, and the error has a range of ±12° at 2.6 GHz and over 20° at 8.45 GHz. The error increases as the DOA shifts away from 0°.

The DOA estimation error is assumed to be the result of several error factors, such as the errors due to inaccuracy in the array element interval, mutual coupling of elements, and plane wave approximation wherein the distance between the transmitting and receiving antennas is small. The inaccuracy in the array element interval and mutual coupling in this measurement are shown in Table 2.3 and, respectively, and the distance between the transmitting and receiving antennas is 3 m. The mutual coupling of elements is measured using a two-port network analyzer. The mutual coupling *MC* is defined by the scattering parameter *S* of the antenna elements as follows:

$$\begin{aligned} &MC_{m_1 m_2} = 20\log_{10}\left|S_{m_1 m_2}\right| \\ &m_1 = 1,\cdots,M \\ &m_2 = 1,\cdots,M \\ &m_1 \neq m_2 \end{aligned} \tag{2.18}.$$

In order to specify a dominant error factor, a numerical analysis including each error (inaccuracy of array element interval, mutual coupling of elements, and plane wave approximation) was performed independently. Independently implies that although the element interval affects the value of mutual coupling in this simulation, the inaccuracy of element interval affects only the change in the reception point assuming that mutual coupling is zero. This mutual relation is discussed in the next chapter. Finally, we independently combine the three error factors, namely, the changes in the reception point, coupling, and the distance, in order to achieve an ideal simulation without an estimation error.

Figure 2.10 shows the DOA estimation error, which includes each of the abovementioned errors. This result indicates that the DOA estimation error resulting from inaccuracies in the array element intervals and mutual coupling is large, and it follows the trend observed in the experimental results in Figure 2.8. On the other hand, the DOA estimation error due to plane wave approximation is small and barely affects the estimation error.

2.3.4 Accuracy of the DOA Estimation Method and Measurement of BER Performance

We measured the accuracy of the DOA estimation method and BER (Bit Error Rate) performance based on the DOA estimation method in the anechoic chamber in an indoor environment. The DBF receiver was used for measurements in the 5 GHz band. The under-sampling method is used for analog to digital conversion, which is a technique used to sample data at a frequency lower than that of IF. The measurement system in the anechoic chamber is shown in エラー! 参照元が見つかりません。(a). Different PN (Pseudo Noise) sequences are transmitted from two points in order to obtain two different signals. The desired and undesired signals are transmitted at a direction of θ_1 and θ_2, respectively. The transmitted power of an undesired wave was fixed and the transmitted power of a desired wave was changed from –20 dB to 0 dB with respect to the undesired wave. The accuracy of the DOA estimation method in the anechoic chamber is shown in エラー! 参照元が見つかりません。(b). The vertical axis represents the absolute value of the DOA estimation error. For each value of SIR (Signal-to-Interference Ratio), the data is obtained 20 times and the estimation error is averaged. As shown in Figure 1, for the BF method, the estimation error increases for SIR values below –10 dB. On the other hand, the estimation error of MUSIC method is less than 1° when SIR = –20 dB. These results indicate that as compared to the BF method, the MUSIC method can estimate the weak signal more

accurately under a strong interfering environment. In an actual environment, these two DOA algorithms exhibit similar DOA estimation errors since an SIR value below –10 dB is not realistic in the propagation environment. In environments where the SIR becomes larger than –10 dB, the BF method is also compatible. Since we verified that the DOA estimation accuracy of the MUSIC method is superior to that of the BF method in the anechoic chamber, we measure the BER performance based on these DOA estimation methods in an indoor environment in the next step. The measurement system in an indoor environment is shown in エラー! 参照元が見つかりません。. The transmitting antenna is placed at both the line-of-sight (LOS) indicated by position 1 and the non-line-of-sight (NLOS) indicated by position 2. The result of DOA estimation by the MUSIC and BF methods is shown in エラー! 参照元が見つかりません。(a). The BER performance when the main beam of the array antenna is rotated from –90° to 90° is shown in エラー! 参照元が見つかりません。(b). The output of the transmitting antenna was minimized and thus the change in the BER performance due to the rotation of the main beam becomes evident. As shown in エラー! 参照元が見つかりません。, at both positions, when the main beam is rotated in the estimated direction, the BER performance improves. The average BER performance with respect to output power at each position is shown in エラー! 参照元が見つかりません。. The information from the DOA method helps determine an optimum beam and better BER performance is obtained for the desired signal. This graph shows that the BER performance based on DOA estimation is approximately 10 dB better than that obtained using a single element of the array antenna. The BF and MUSIC methods result in almost equivalent BER performance, which is similar to that obtained by the MMSE method. These results indicate that the BF method can effectively steer a beam based on DOA estimation and also in an indoor propagation environment.

2.4 Conclusion

In this chapter, we formulated the array antenna and DOA estimation and explained prototype array antenna systems. An evaluation method using a rotating array antenna was proposed. We analyzed the error factor based on experiments conducted in the anechoic chamber. We evaluated the array antenna system using DOA estimation, and on the basis of this evaluation, we clarified the problems related with the hardware and propagation environment of the array antenna system. The DOA estimation error is large due to errors from inaccuracies in the array element intervals and mutual coupling. These errors are not independent, and they vary with the antenna structure and machining accuracy. We will examine these errors in detail in the following chapters.

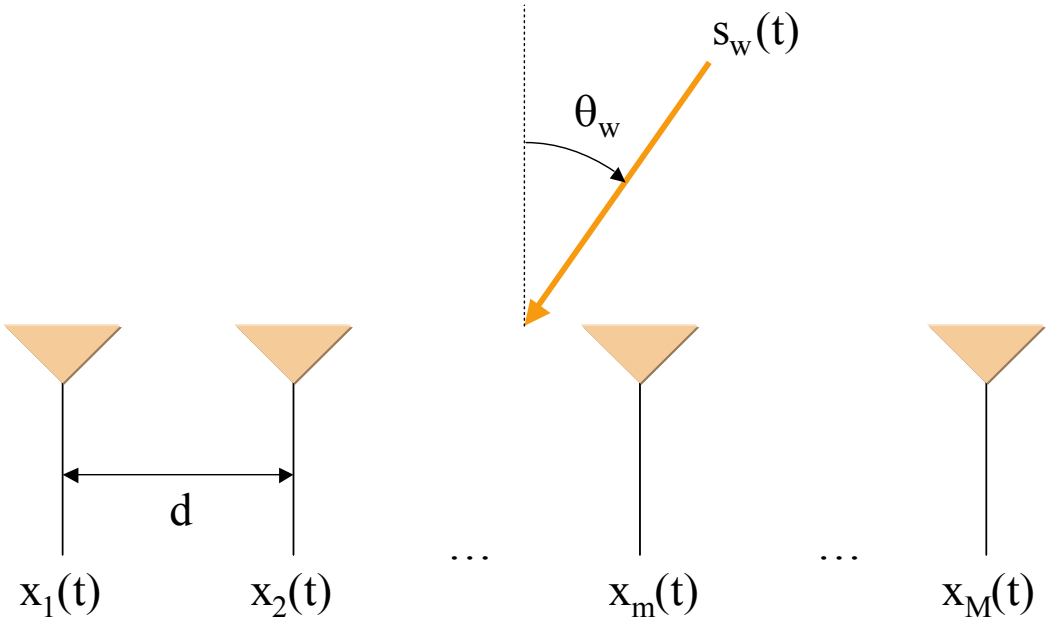

Figure 2.1: Array antenna geometry.

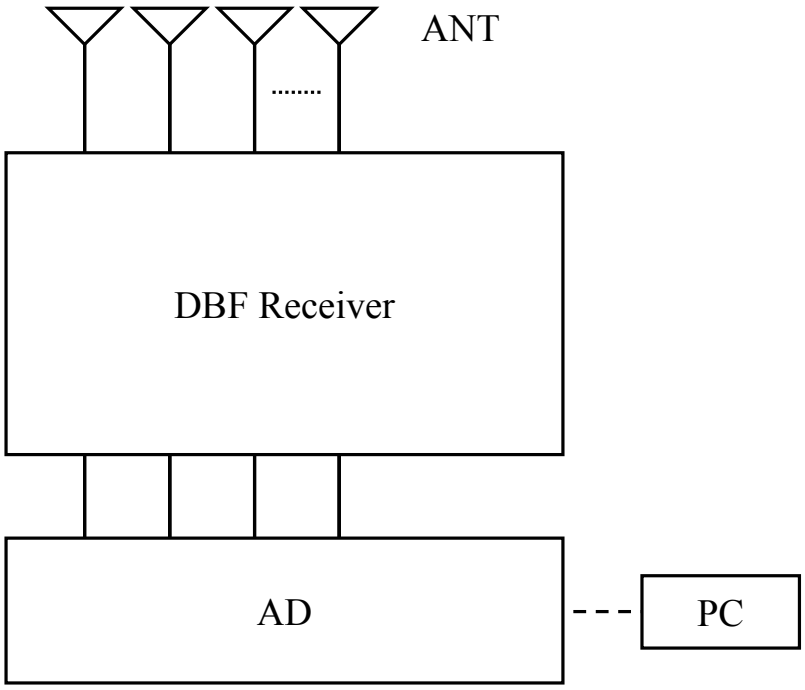

Figure 2.2: Composition of the DBF array antenna.

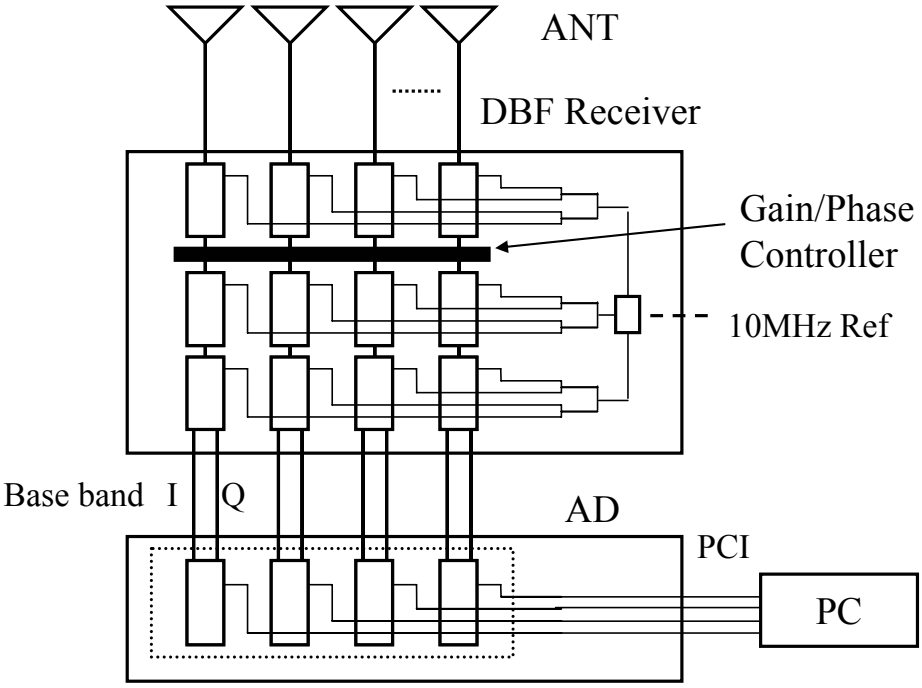

Figure 2.3: Composition of the DBF array antenna (initial).

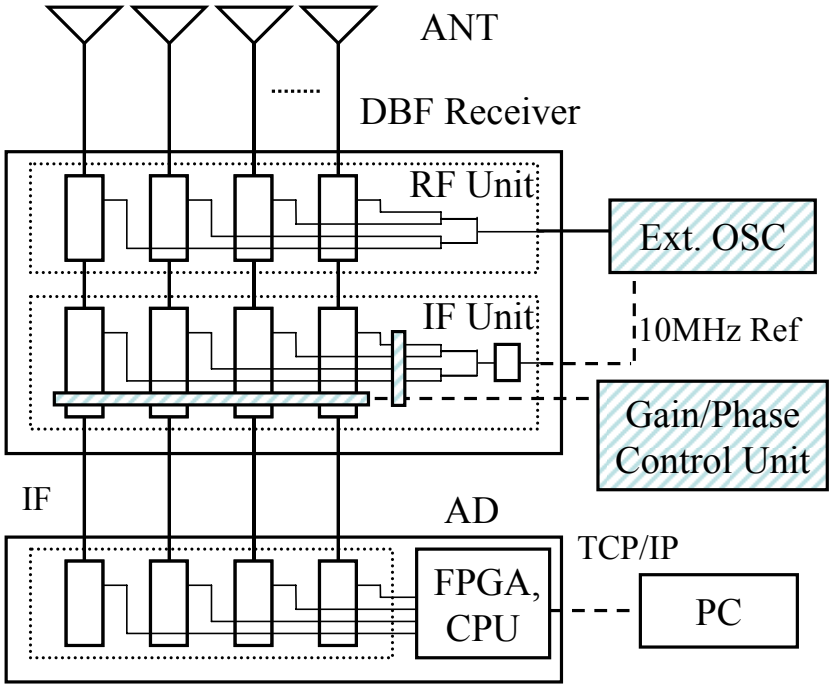

Figure 2.4: Composition of the DBF array antenna (after improvements).

Figure 2.5: 2~8 GHz 4-channel YTF transmitter and receiver.

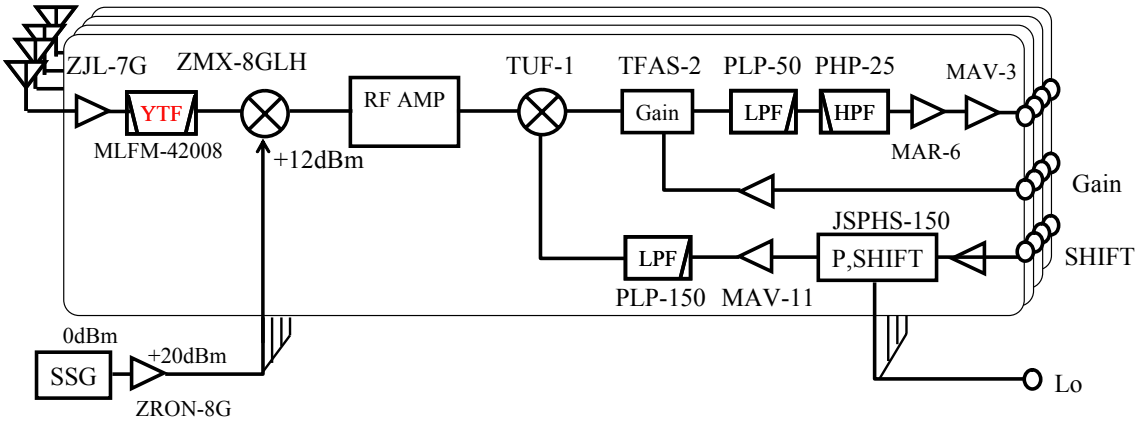

Figure 2.6: Block diagram of the 2-8 GHz 4-channel YTF receiver.

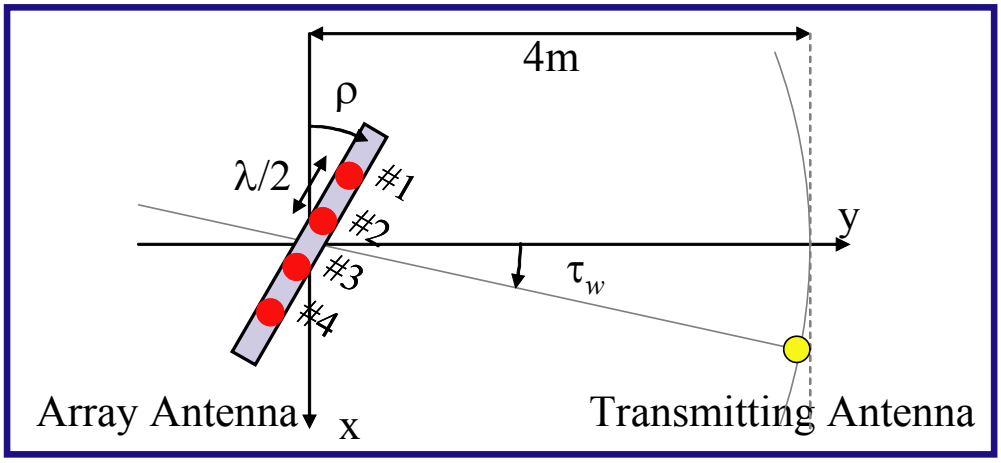

Figure 2.7: Evaluation of the array antenna system.

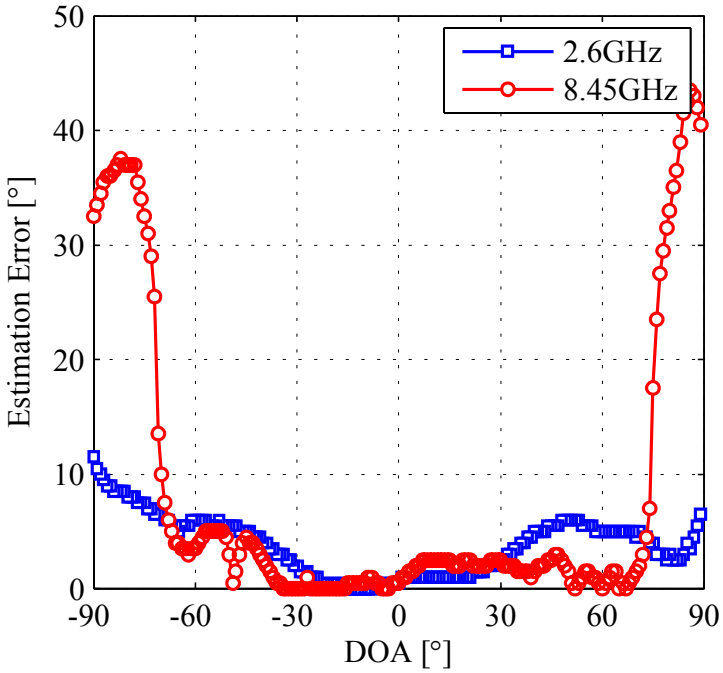

Figure 2.8: Estimation error (measurement).

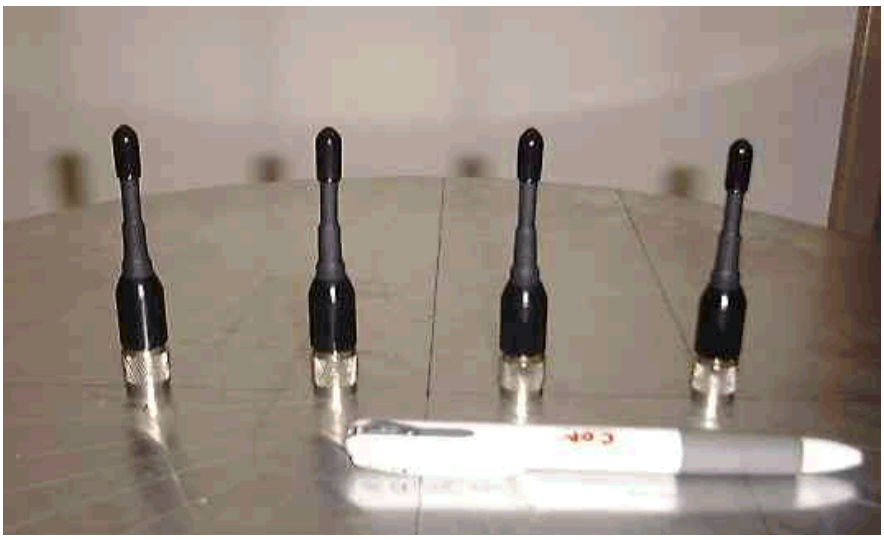

(a) 2.6 GHz

(b) 8.45 GHz

Figure 2.9: Array antenna.

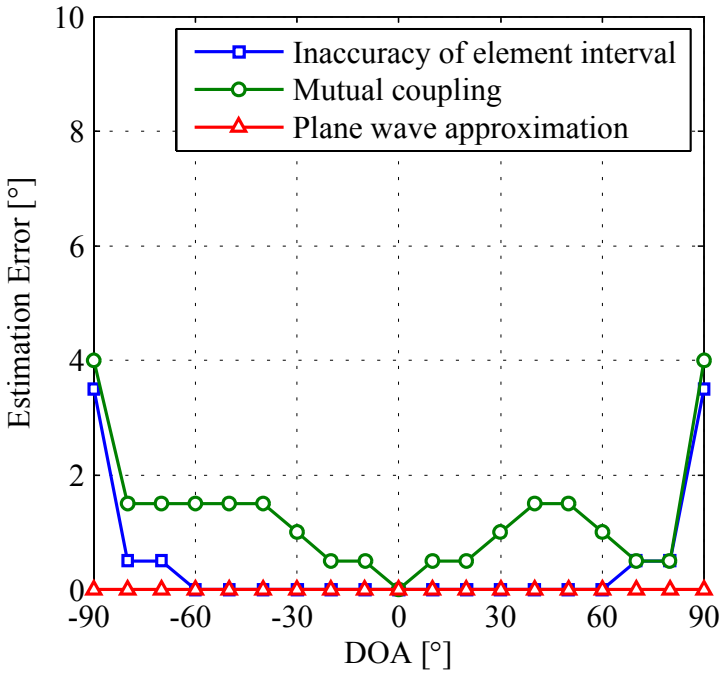

Figure 2.10: Estimation error (simulation).

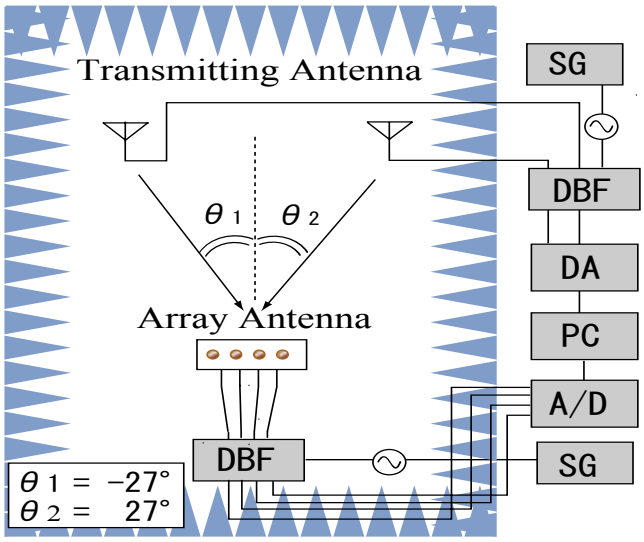

(a) Measurement system

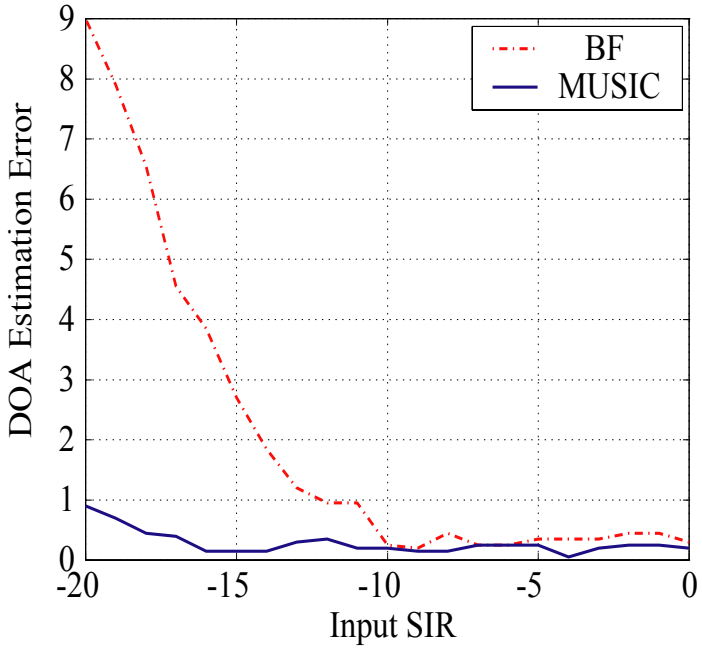

(b) Accuracy of the DOA estimation

Figure 2.11: The measurement system and accuracy of DOA estimation in the anechoic chamber.

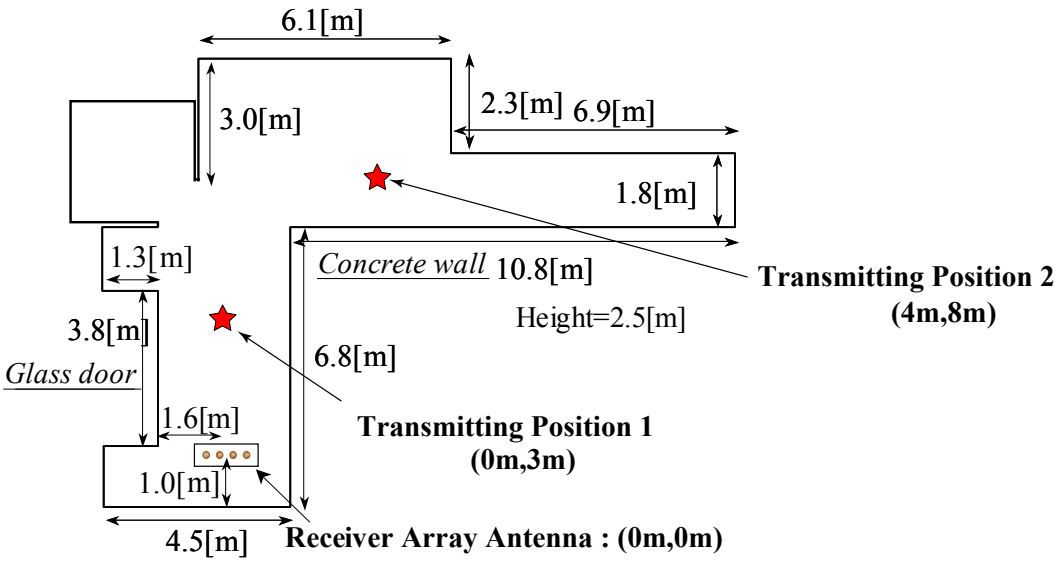

Figure 2.12: The measurement system in an indoor environment.

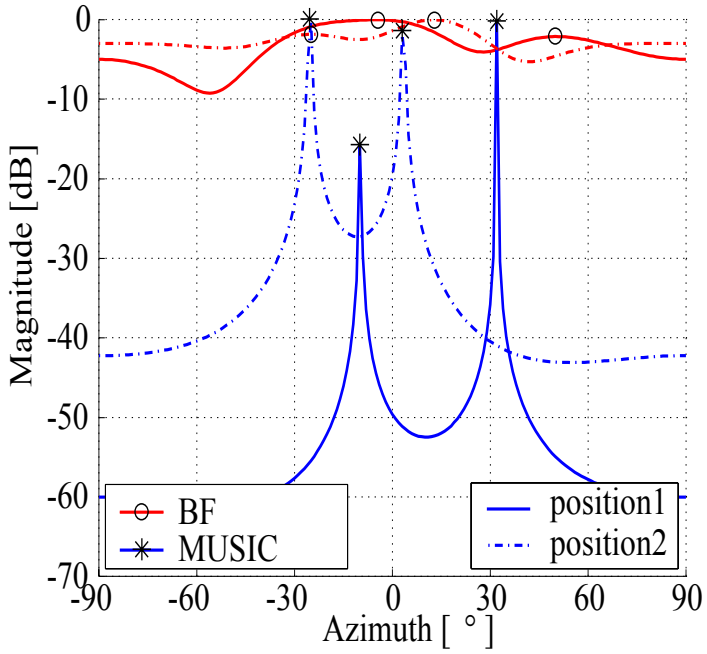

(a) DOA estimation

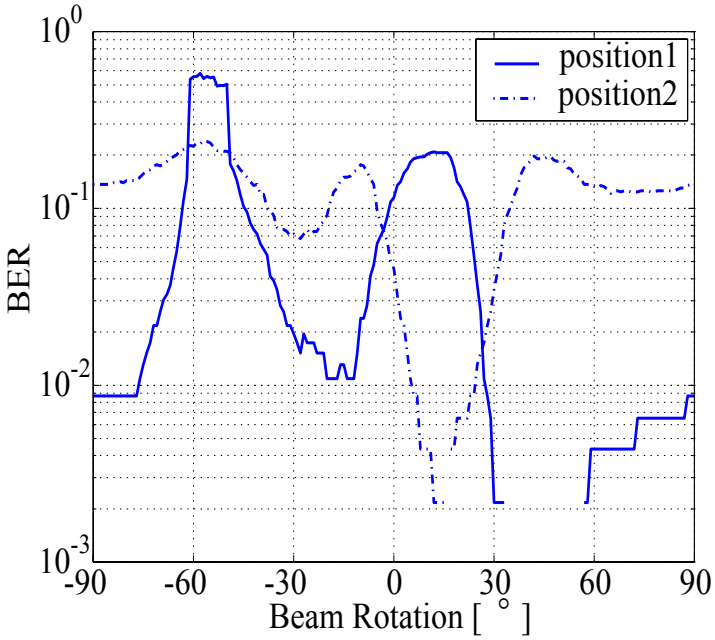

(b) BER performance by steering the beam

Figure 2.13: DOA estimation and BER performance by steering the beam in an indoor environment.

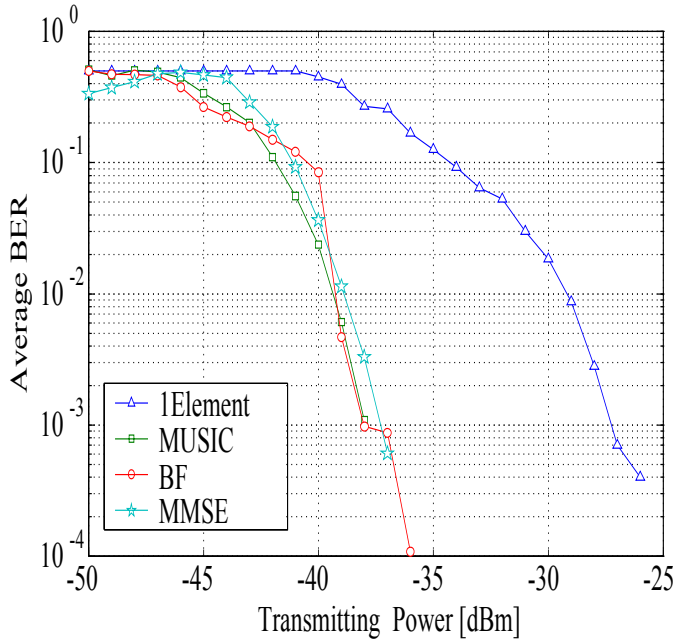

Figure 2.14: BER performance with respect to the output power in an indoor environment.

Table 2.1: Characteristics of the prototype DBF receiver.

Number	Carrier frequency [GHz]	Output	LO oscillator	Remote phase and amplitude adjustment controller	Number of channels	Band width
1	2.665	I, Q	Inside	No	4	128 kHz
2	8.45	I, Q	Outside	Yes	8	10 MHz
3	8.45	IF (10 MHz)	Outside	Yes	8	10 MHz
4	2-8	IF (40 MHz)	Outside	Yes	4	10 MHz
5	2-8	IF (40 MHz)	Outside	Yes	8	10 MHz

Table 2.2: Characteristics of the prototype array antenna.

Carrier frequency	Element spacing error margin	Interconnection between elements
2.6 GHz	Within $\pm 6.2 \times 10^{-3}$	–14 dB or less
8.45 GHz	Within $\pm 6.2 \times 10^{-2}$	–13 dB or less

Table 2.3: Inaccuracies in the element intervals at 2.6 GHz ($\lambda/2 = 5.624 \times 10^{-2}$ m).

#1	0 (standard)
#2	–0.0049λ
#3	–0.0062λ
#4	–0.0030λ

Table 2.4: Mutual coupling between the elements at 2.6 GHz.

S12	–27 dB
S13	–28 dB
S14	–32 dB
S23	–14 dB
S24	–34 dB
S34	–26 dB

Chapter 3

Quantitative Analysis of the Array Antenna System

3.1 Introduction

In this chapter, we conduct a detailed examination of the errors due to inaccuracy in array element positions, mutual coupling of elements, and plane wave approximation wherein the distance between the transmitting and receiving antennas is small. Element position and mutual coupling influence each other and affect the array antenna element pattern. First, we formulated the array antenna that takes into account the effects of the antenna element pattern and used the moment method to quantitatively and statistically analyze mutual coupling and DOA estimation error. The DOA estimation error is dependent on the null steering of the adaptive antenna. Next, changing simulation is performed by varying the extent of mutual coupling. It is impossible to realize an antenna without any coupling; however, the coupling can be suppressed. This property will be useful in manufacturing the array antenna.

3.2 Quantitative Analysis of Hardware Problems

3.2.1 Formulation of the Array Antenna

In this section, an array antenna model that takes into account the effects of the array antenna pattern is described. The complex pattern in the horizontal plane of each array antenna element is expressed as $p_m(\theta)$. The output of each array element $x_m(t)$ is given by the following expression

$$x_m(t) = \sum_{w=1}^{W} \left\{ s_w(t)\, p_m(\theta_w) \exp\left(j(m-1)\frac{2\pi}{\lambda} d \sin\theta_w \right) \right\} + n_m(t) \tag{3.1}$$

It is thought that the amplitude and phase of the steering vector vary on the basis of the pattern of the vector expression. The steering vector is expressed by the following equation

$$\mathbf{a}(\theta_w) = \left[p_1(\theta_w) \quad p_2(\theta_w)\exp\left(j\frac{2\pi}{\lambda} d \sin\theta_w \right) \quad \cdots \quad p_M(\theta_w)\exp\left(j(M-1)\frac{2\pi}{\lambda} d \sin\theta_w \right) \right]^T \tag{3.2}.$$

3.2.2 Evaluation Method

The relation between mutual coupling, array manufacturing error, and the DOA estimation error is examined by a numerical analysis of DOA estimation using the

model and by considering the element pattern. Here, the array antenna is a uniform linear array antenna consisting of a 4-element dipole antenna arranged in parallel with half-wavelength intervals. The element pattern is calculated by the moment method. In addition, the distance between the transmitting antenna and the receiving array antenna is assumed to be sufficiently large and the arriving signal is a plane wave. Figure 3.1 shows the relation between the element interval and mutual coupling of the 4-element linear array antenna calculated by the moment method. The mutual coupling is approximately –15 dB in the half-wavelength interval. The array element position was given by the two-dimensional normal distribution that existed with radius r and a probability of 99.7%, as shown in Figure 3.2. The number of trials for each condition was 100.

3.2.3 Mutual Coupling and Manufacturing Error

The radius r was varied for five conditions: 0λ, $0.5 \times 10^{-2}\lambda$, $1.0 \times 10^{-2}\lambda$, $1.5 \times 10^{-2}\lambda$, and $2.0 \times 10^{-2}\lambda$. Figure 3.3 shows the median *EM*, standard deviation *ES*, and the range *ER* (difference between the maximum and minimum values) of the absolute value of the DOA estimation error for each direction.

The condition $r = 0$ represents no manufacturing error; *EM* can assume a maximum value of 2.4°, and it does not become 0°. In addition, the error changes depending on the DOA because the array element pattern was changed by mutual coupling. Figure 3.4 shows the array element pattern with $r = 0$. Each value is standardized based on the value of each element at 0°. The difference in amplitude and phase dispersion is approximately 5 dB and 30°, respectively, which affects the estimation error. When r increases, *EM* increases irregularly in almost every DOA. This shows that the effect due to element position error is non-linear.

In the condition $r = 0$, *ES* and *ER* for every DOA were automatically 0°.

When r increases, *ES* and *ER* increase gradually. With regard to the DOA axis, *ES* and *ER* increased rapidly around 70°. This is because the aperture of a linear array antenna narrows at approximately 90° and the error distribution does not follow normal distribution. On the other hand, for the condition below 70°, the dispersion follows normal distribution; therefore, *ER* and *ES* can be suppressed when r is sufficiently small.

The radius r was then set to a smaller value and the similar simulations were performed by varying r for the following five conditions: 0, $0.1 \times 10^{-2}\lambda$, $0.2 \times 10^{-2}\lambda$, $0.3 \times 10^{-2}\lambda$, and $0.4 \times 10^{-2}\lambda$. Figure 3.5 shows the median *EM*, standard deviation *ES*, and the range *ER* of the absolute value of the DOA estimation error for each direction. The tendency was similar to that in the previous simulation and the dispersion was marginally suppressed. In particular, when r is set to $0.1 \times 10^{-2}\lambda$, *ER* decreases to below 0.5° for a DOA that is less than 60° and the dispersion is almost negligible. The value $0.1 \times 10^{-2}\lambda$ corresponds to 35.5 μm and 112 μm at 8.45 GHz and 2.665 GHz, respectively.

3.2.4 Varying the extent of Mutual Coupling

The estimation error is examined by changing the parameters of the scattering matrix and element numbers by computer simulation. The error at approximately 90° increases considerably due to a linear array; hence, the maximum error E_{max} is selected from the DOA between 0° to 60° at 10° intervals. The direction of 0° represents the broad-side direction of the array. The element number M is varied from 4 to 20 for every 4 elements. Figure 3.6 shows this condition.

Figure 3.7 shows the setting of scattering matrix S. S is assumed to be a Toeplitz matrix and we neglect the noise matrix N. The first column $\mathbf{s}$ is defined as

$$\boldsymbol{s} = \left[A_1 e^{j\phi_1} \quad A_2 e^{j\phi_2} \quad \cdots \quad A_M e^{j\phi_M} \right] \tag{3.3}$$

It is assumed that the return loss of the element A_1 was –14 dB. The mutual coupling with A_2 is changed from –10 dB to –50 dB and the coupling with other elements $A_{3,4,\ldots,M}$ is inversely proportional to the distance between the elements.

$$A_n = \frac{A_2}{n-1} \quad \text{n=2, 3,…,M} \tag{3.4}$$

The phases $\varphi_{1,2,\ldots,M}$ of $\boldsymbol{s}$ are uniform random numbers. The amplitude and phase of N follow normal distribution and the standard deviation is denoted by NA_{std} and $N\varphi_{std}$, respectively.

Figure 3.8 shows the maximum value of the estimation error E_{max} as a function of mutual coupling with A_2. In this simulation, NA_{std} and $N\varphi_{std}$ are 1 dB and 5°, respectively, and the SNR is 20 dB. E_{max} decreases steeply from A_2 = –10 dB to –30 dB and fluctuates thereafter. Figure 3.9 shows E_{max} as a function of NA_{std}. $N\varphi_{std}$ is set to NA_{std} [dB] × 5°. E_{max} becomes greater than 1° when NA_{std} and $N\varphi_{std}$ are 1 dB and 5°, respectively. As evident from the above example, the estimation error is minimized when $A_2 \leqq$ –30 dB, $NA_{std} \leqq$ 1 dB, and $N\varphi_{std} \leqq$ 5°.

3.3 Numerical Analysis of Environmental Problems

3.3.1 Formulation of the Array Antenna

In this section, an array antenna model that takes into account the effects of

the distance between the transmitting antenna and the receiving array antenna is described. In this situation, the incoming wave is not assumed to be a plane wave and the DOA of each array element is different, as shown in Figure 3.10. The distance from the center of the array to the transmission source is defined as L_w and the DOA with respect to the center of the array is defined as θ_w. The output of each array element $x_m(t)$ is then given by the following expression:

$$x_m(t) = \sum_{w=1}^{W} s_w(t) \exp\left(j \frac{2\pi}{\lambda} \Delta L_m \right) + n_m(t) \tag{3.5}$$

where ΔL_m is the difference in the distance between each element and the transmitting antenna with respect to the center of the array antenna and is defined by the following expression:

$$\Delta L_m = L_w - \sqrt{\left[L_w \sin\theta_w - \xi_m \right]^2 + L_w{}^2 \cos^2 \theta_w} \tag{3.6}$$

$$\xi_m = d(m-1) - \frac{d(M-1)}{2} \tag{3.7}$$

The difference in the steering vector is caused due to the variation in the phase and amplitude in the vector expression

$$\mathbf{a}(\theta_w) = \left[1 \quad \exp\left(j \frac{2\pi}{\lambda} \Delta L_2 \right) \quad \cdots \quad \exp\left(j \frac{2\pi}{\lambda} \Delta L_M \right) \right]^T \tag{3.8}.$$

3.3.2 Distance between Transmitting and Receiving Antennas

The relation between the distance separating the transmitting and receiving array antennas and the DOA estimation error is examined by a numerical analysis of DOA estimation using the model that considers distance. The DOA is varied within the range of ±90° at intervals of 1° and *EA* is the maximum value of the absolute value of the estimation error. The relation between the distance separating the transmitting antenna L_1 and the receiving antenna *EA* is shown in Figure 3.11. *EA* is inversely proportional to the second power of L_1. The estimation error becomes less than 0.1° if L_1 is greater than approximately 10λ and the influence of distance between the transmitting antenna and the receiving array antenna can almost be disregarded. The value 10λ corresponds to 35.5 mm and 112 mm at 8.45 GHz and 2.665 GHz, respectively.

3.4 Conclusion

In this chapter, we conducted a detailed examination of errors due to inaccuracy in array element positions, mutual coupling of elements, and plane wave approximation wherein the distance between transmitting and receiving antennas is small. First, we formulated the array antenna that takes into account the effects of the antenna element pattern and used the moment method to quantitatively and statistically analyze mutual coupling and the DOA estimation error. When the inaccuracy of the array element position at a radius of $0.1 \times 10^{-2}\lambda$ is within 99.7%, the DOA estimation error decreases to below 0.5° for a DOA that is less than 60° and the dispersion was negligible. The value $0.1 \times 10^{-2}\lambda$ corresponds to 35.5 μm and 112 μm at 8.45 GHz and 2.665 GHz, respectively. Next, changing simulation was carried out by varying the

extent of mutual coupling. The estimation error is minimized when the mutual coupling between neighboring elements is –30 dB and the dispersion of the amplitude and phase in the element's pattern is within 1 dB and 5°, respectively. The influence of the distance between the transmitting and receiving array antennas is less than 0.1° when the distance is greater than approximately 10λ. The distance of 10λ corresponds to 35.5 mm and 112 mm at 8.45 GHz and 2.665 GHz, respectively.

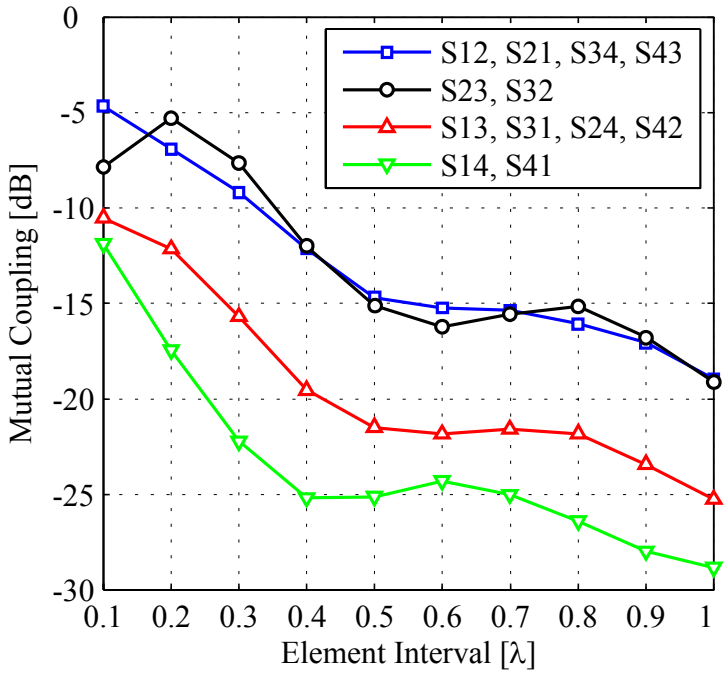

Figure 3.1: Mutual Coupling of a 4-element dipole array (moment method).

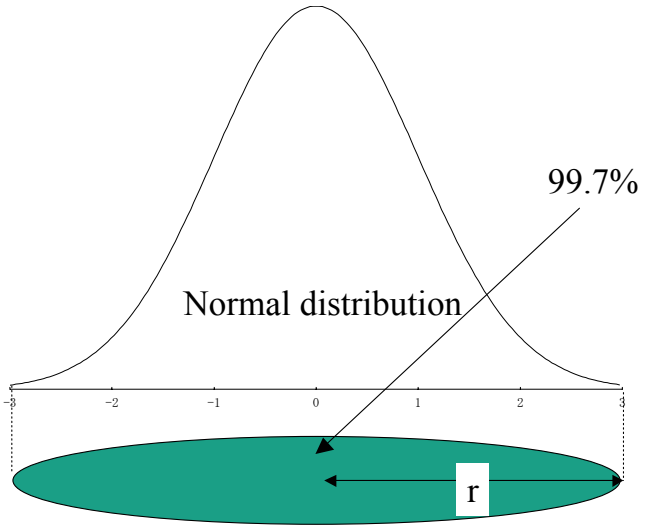

Figure 3.2: Error in element position (2-D normal distribution).

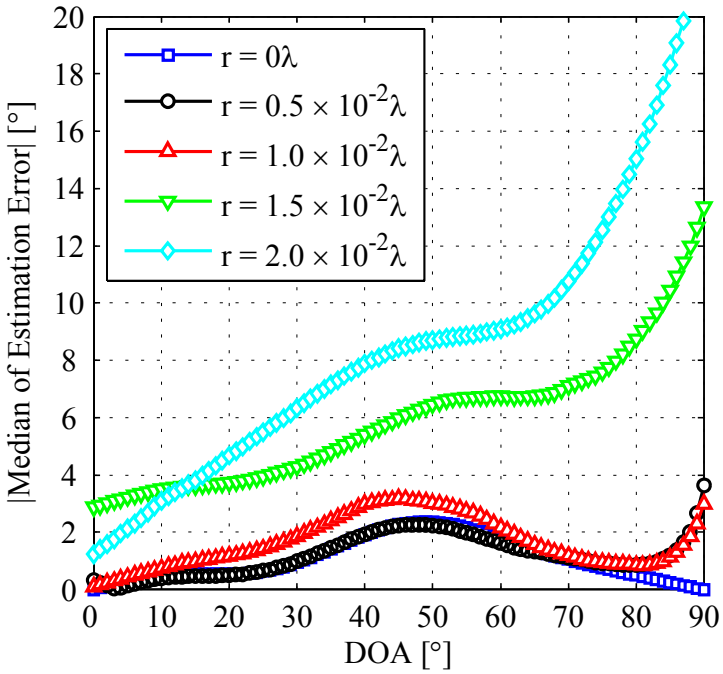

(a) Absolute value of median of estimation error

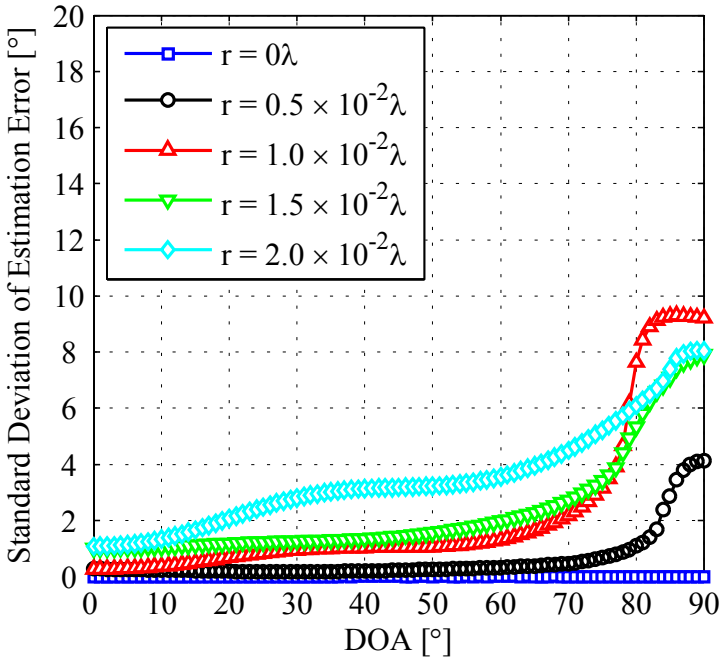

(b) Standard deviation of estimation error

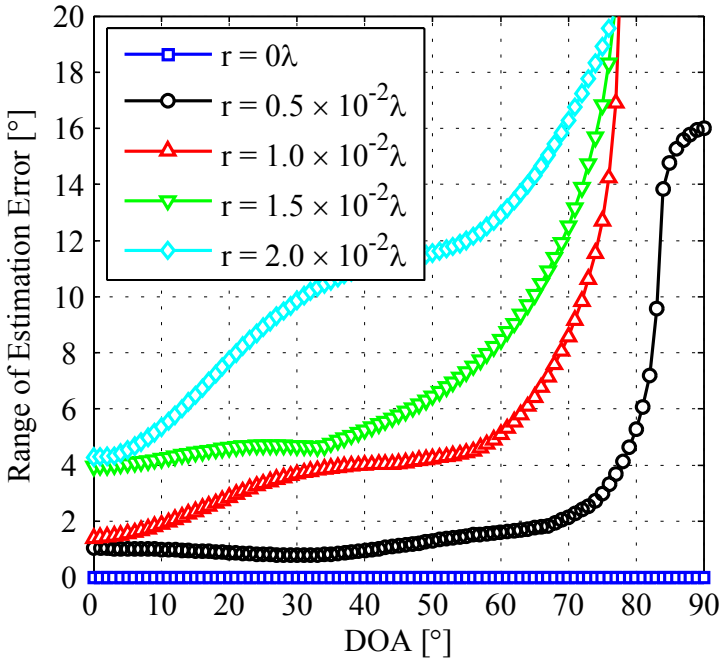

(c) Range of estimation error

Figure 3.3: Estimation error as a function of DOA (simulation).

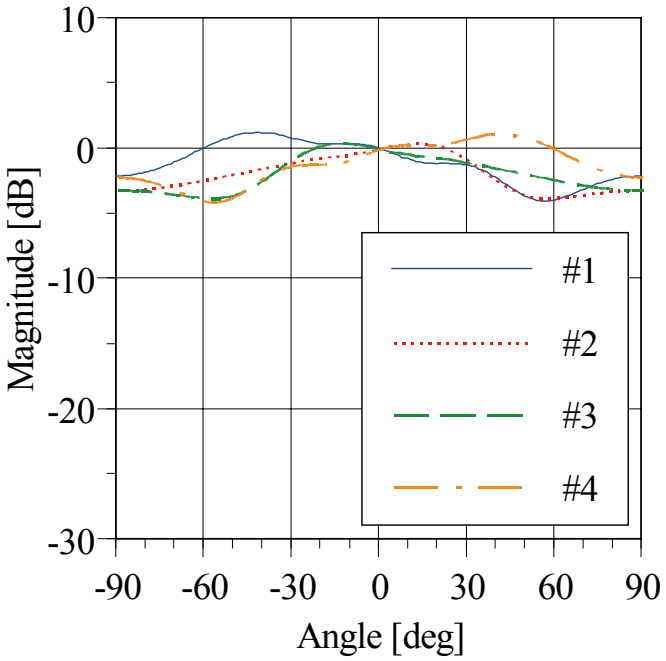

(a) Amplitude

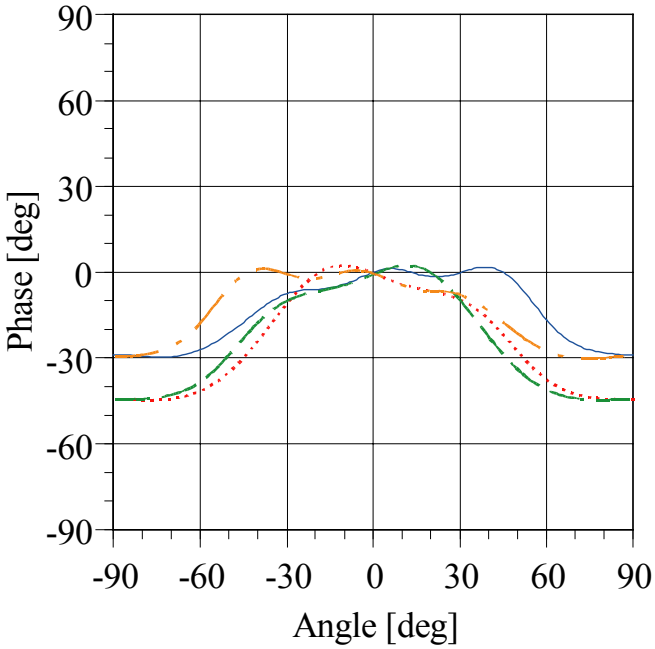

(b) Phase

Figure 3.4: Element pattern of a 4-element linear array (moment method).

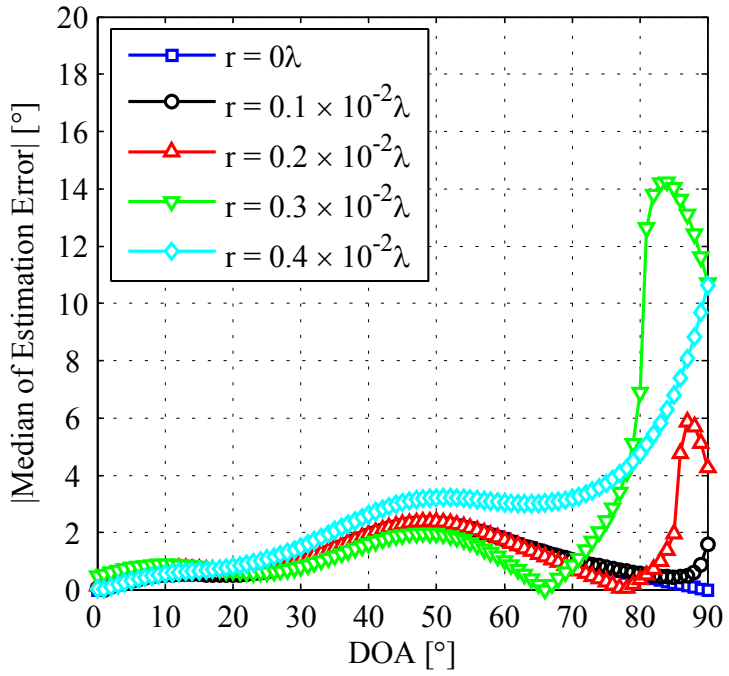

(a) Absolute value of median of estimation error

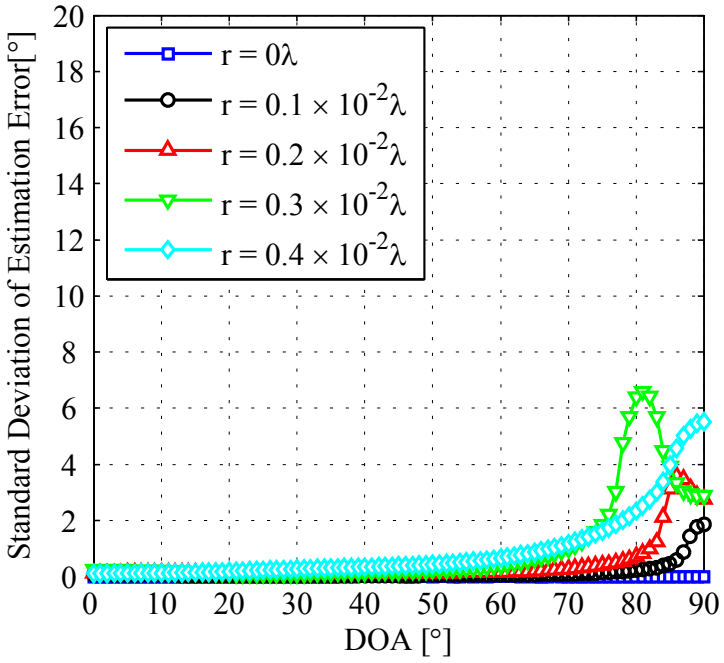

(b) Standard deviation of estimation error

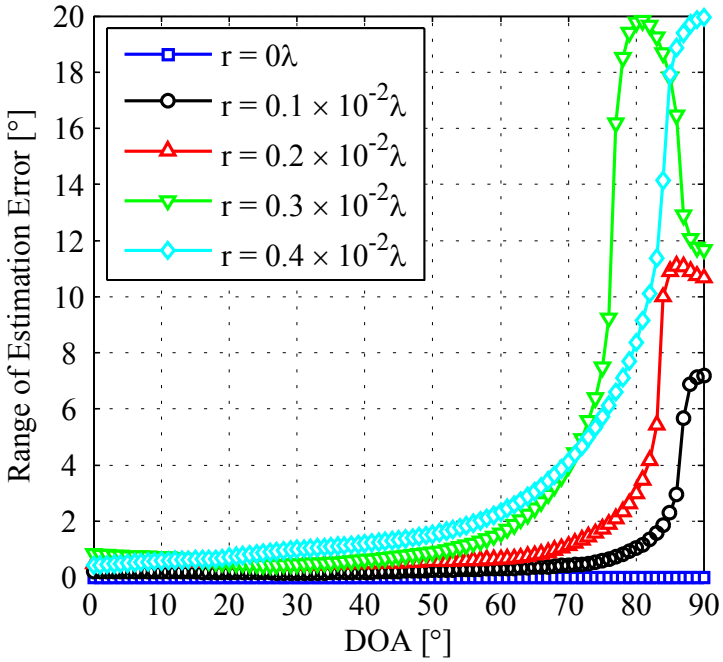

(c) Range of estimation error

Figure 3.5: Estimation error as a function of DOA (simulation).

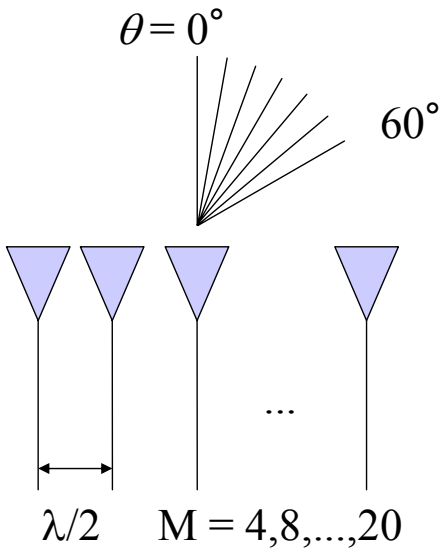

Figure 3.6: Array antenna and direction.

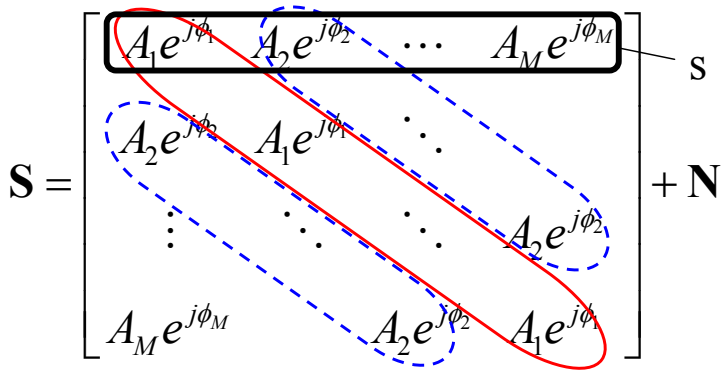

Figure 3.7: Scattering matrix.

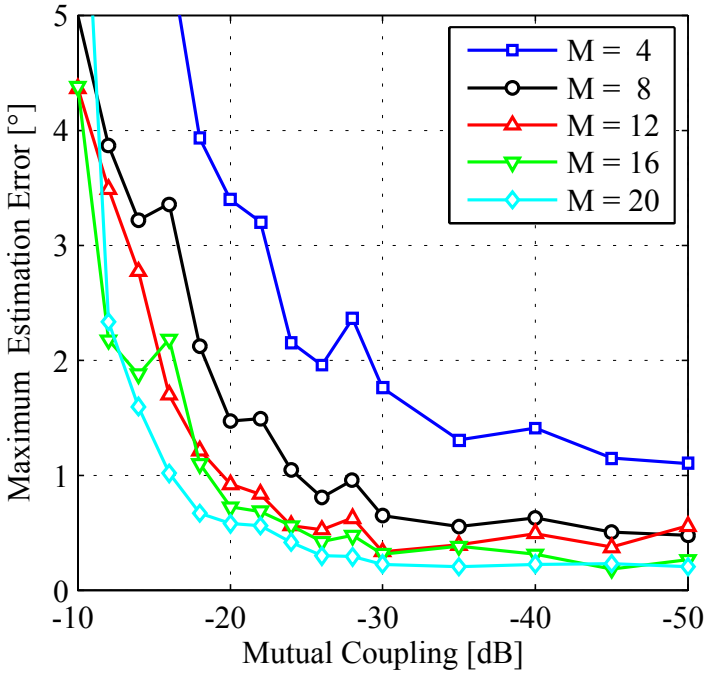

Figure 3.8: Maximum value of estimation error as a function of mutual coupling (NA_{std}: 1 dB, $N\varphi_{std}$: 5°) (simulation).

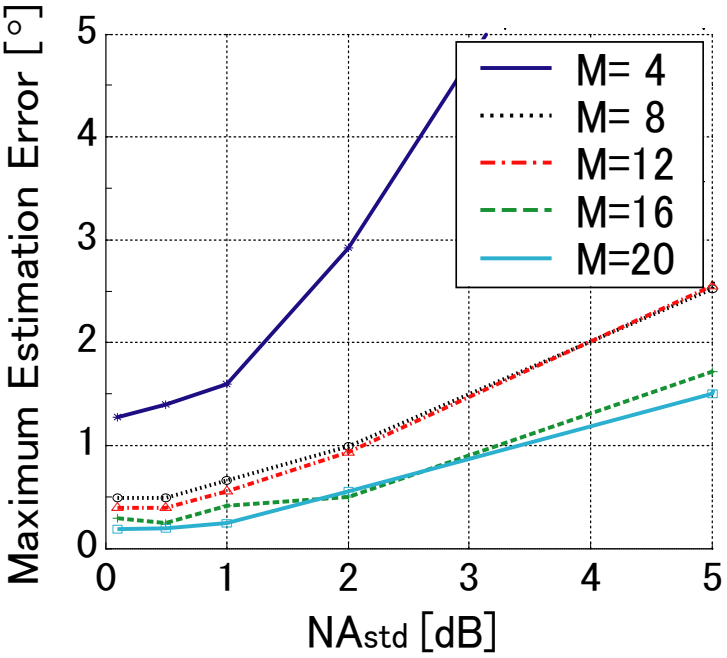

Figure 3.9: Maximum value of estimation error as a function of NA_{std} (A_2: –30 dB) (simulation).

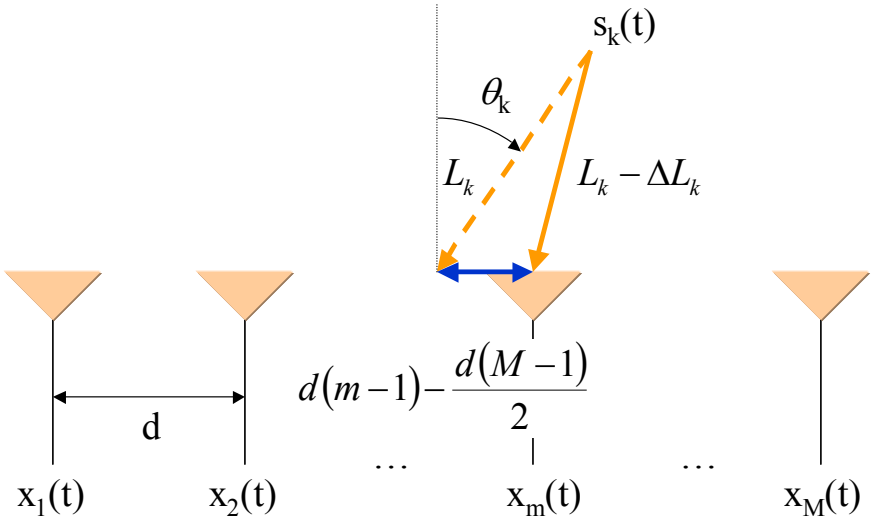

Figure 3.10: Model that considers the distance between the transmitting and receiving antennas.

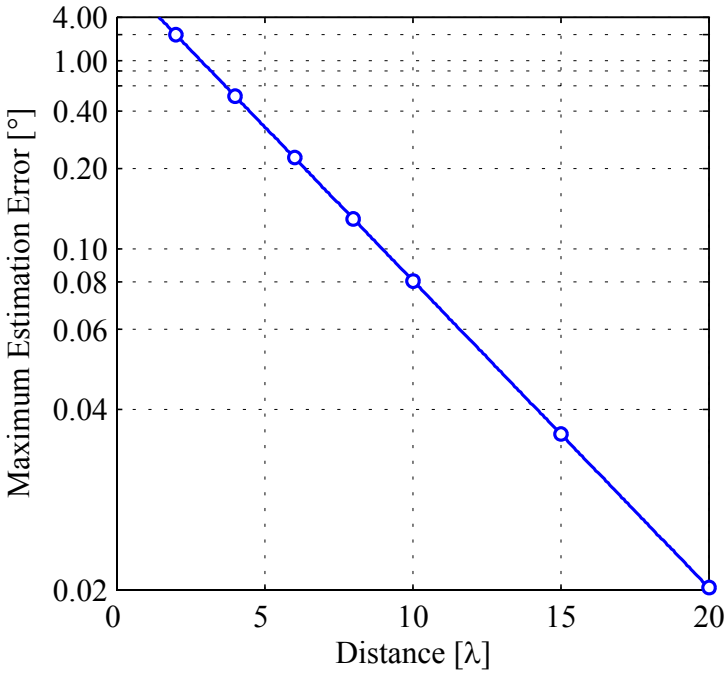

Figure 3.11: Distance between the transmitter and receiver and the maximum value of estimation error (simulation).

Chapter 4

High-Precision Array Antenna System

4.1 Introduction

In this chapter, we propose a calibration method for suppressing the error factors examined in Chapter 2 and 3. The calibration of the array antenna system is related to modeling. In mobile communication, a system that can be calibrated during operation is key to adaptive antenna implementation based on array antenna systems. For such systems, the method for calibrating the device or including the antenna is proposed; however, a mutual coupling calibration system is necessary when the antenna elements are few in number. The steering vector compensation method is the most basic calibration method. However, this method is only applicable to algorithms that use the steering vector and SSP method and measurements in the anechoic chamber are required for calibration. Coupling calibration using a fixed calibration antenna can eliminate these problems, and it can be calibrated during operation. In this calibration method, which employs coupling compensation method, determining the calibration antenna element position is important since this affects the accuracy of calibration. The calibration of mutual coupling is often studied at the receiving end because it is easy to perform measurements at the receiving end and the principles used at the receiving end can be applied to the transmitting end by orthogonalization. However, the calibration of the transmitting array antenna is important for an FDD adaptive array system, and it is

difficult to construct such a calibration system. The correlation matrix estimation method for the transmitting array antenna is demonstrated experimentally in the anechoic chamber. In addition, the time of calibration of the pattern is reduced by employing the element interval tuning method and a low-coupling array antenna system based on the discussion in Chapter 3. The array antenna element pattern changes due to several error factors; however, optimum adjustment of the element interval, mutual coupling, and number of elements leads to the achievement of a high-precision array antenna system with reduced errors.

4.2 Calibration Method for Mutual Coupling

4.2.1 Steering Vector Compensation Method

In order to compensate for the DOA estimation errors resulting from array manufacturing errors or mutual coupling, the steering vector compensation method, which uses a measured steering vector for DOA estimation or for the adaptive array antenna, is the most basic calibration method. This method has a limitation, that is, it is only applicable to algorithms that use the steering vector. The measured steering vector includes a phase difference and relative amplitude ratio for the standard element in each direction. The array manufacturing error and mutual coupling can change the ideal array steering vector.

We tested two measurement methods. In one method (method C1), the entire array antenna system is used. In the case of one transmitting antenna (W = 0), the received signal of each element is

$$x_m(t) = s(t) \cdot a_m(\theta) + n_m(t) \quad .$$

After averaging the signal to reduce the noise component, the steering vector is expressed as follows:

$$a_m(\theta) = \frac{x_m}{s} \quad .$$

However, the absolute phase difference between s and x_m cannot be measured, and $a_m(\theta)$ cannot be calculated from the above equation. The steering vector can be obtained by using the relative value of the inter-element spacing; hence, standardization by the first element can be expressed as follows:

$$a_m(\theta) = \frac{x_m}{x_1}$$

In the second method (method C2), only the antenna part is used to measure the element pattern of the array antenna. The existing pattern measurement system is a viable option for both this calibration and separate calibration with the receiver. In this method, the absolute phase difference between s and x_m can be measured; however, the measurement can only be performed on a single element at a time.

The comparison of the estimation error before and after calibration by the C1 and C2 methods at 2.6 GHz and 8.45 GHz for the array antenna system is shown in Figure 4.1. It confirms that the errors decreased in almost all directions. C1 and C2 exhibit almost identical improvements. It is observed that the steering vector measured by the experiment was effective in both methods. In addition, we used the interpolation of the thinned-mode vector in order to reduce a measurement point. Figure 4.2 shows

the estimation error obtained using the interpolated mode vector by the spline interpolation method. Interpolation occurs at intervals of 10°, 20°, and 30°. In the case of the 30° interval, the error displays a significant increase; hence, it is not shown in Figure 4.2. At 10° intervals, the estimation error is ±3°, which is very effective and is identical to that observed in case without interpolation. In the case of the 20° interval, the estimation error is ±5° and is not as significant as that before compensation. The estimation error for the 30° interval is ±19° and is unsuitable for correction data. Based on the above, the interpolation is effective up to the 20° interval.

4.2.2 Calibration System of the Transmitting Array Antenna

The calibration of mutual coupling is often studied at the receiving end because it is easy to perform measurements at the receiving end and the principles for the receiving end can be applied to the transmitting end by orthogonalization. However, calibration of the transmitting array antenna is important for the FDD adaptive array system, and the construction of such a calibration system is difficult. In this section, the correlation matrix estimation method for the transmitting array antenna is demonstrated experimentally in the anechoic chamber. In particular, the synchronous cable for sending and receiving signals becomes redundant with the installation of the omnidirectional antenna in the vertical direction of the transmitting array antenna.

The transmitting signal s is diffused into M orthogonal signals; it is then transmitted with each weight vector $\boldsymbol{w}$ and multiplexed. The transmitted signal is received at point w and is diffused back to vector $\boldsymbol{x}(\theta)$; $\boldsymbol{a}(\theta)$ is the steering vector of each direction of the transmitting array. The coupling matrix of the transmitting antenna is defined as $\boldsymbol{K}$ in the following expression:

$$\mathbf{X} = \frac{1}{N}\mathbf{A} \cdot \mathbf{K} \cdot \mathbf{W} \cdot s + \mathbf{n} \tag{4.1}$$

where

$$\mathbf{X}=\left[\mathbf{x}(\theta_1)\quad \mathbf{x}(\theta_2)\quad \cdots\quad \mathbf{x}(\theta_w)\right]^T \tag{4.2}$$

$$\mathbf{A}=\left[\mathbf{a}(\theta_1)\quad \mathbf{a}(\theta_2)\quad \cdots\quad \mathbf{a}(\theta_w)\right]^T \tag{4.3}$$

$$\mathbf{W}=\left[\mathbf{w}_1\quad \mathbf{w}_2\quad \cdots\quad \mathbf{w}_M\right] \tag{4.4}$$

and ***n*** is the noise procession. ***K*** is represented in the following expression by the minimum mean square method from equation (4.1). The symbol + indicates the Moore and Penrose generalization inverse matrix.

$$\mathbf{K}=\frac{N}{s}\mathbf{A}^{+}\cdot(\mathbf{R}-\mathbf{n})\cdot\mathbf{W}^{+} \tag{4.5}.$$

Initial deviation and mutual coupling of the array antenna can be corrected by introducing the inverse matrix of K in the transmission signal in advance.

Figure 4.3 shows the experimental system. The modulation scheme used is QPSK with 64 M-sequence symbols as the six orthogonal codes. The phase standard was transmitted from an omnidirectional antenna arranged above the center element. Figure 4.5 and show the various patterns before and after calibrating with the above method. It can be confirmed that the calibration is performed correctly.

4.2.3 Coupling Calibration System using a Fixed Calibration Antenna

Figure 4.7 shows the coupling calibration system using a fixed calibration

antenna. This calibration system can be used when the array antenna system is in operation, and it can be effectively used in systems that require sequential calibration during operation such as the base station antenna for mobile communications. Determining the calibration antenna element position is the key to this system since it affects the accuracy of calibration.

The DOA estimation error of the MUSIC method is examined by a numerical analysis that varies the position of the calibration antenna element (θ_{in} and θ_{out}) and the vertical angle α of the transmitting antenna. In this simulation, the pattern of each element is calculated by the moment method. The source signal is a sine wave, the SNR is 20 dB, and the number of samples for reception is 100. Figure 4.8 shows the simulation results obtained by varying θ_{in} and θ_{out}. In order to ensure error reduction, the best position of the calibration antenna is $\theta_{in} = 15°$ and $\theta_{out} = 45°$ wherein the estimation error is within 0.8°. Figure 4.9 shows the estimation error by varying α for $\theta_{in} = 15°$ and $\theta_{out} = 45°$. When $\alpha < 40°$, the estimation error is within 0.5°. Figure 4.10 shows the estimation error measured before and after calibration. The transmitting antenna is set to $\theta_{in} = 15°$ and $\theta_{out} = 45°$ and $\alpha = 20°$ and 40°. The calibration is effective and it reduces the estimation error. The estimation error was suppressed within 1° at $\theta_{in} = 15°$ and $\theta_{out} = 45°$ and $\alpha = 40°$ when DOA < 60°.

4.3 High-Precision Array Antenna System

4.3.1 Element Interval Tuning Method

In algorithms using the steering vector, mutual coupling and pattern distortion can be included by using the measured steering vector as shown in section

4.2.1. On the other hand, algorithms such as ESPRIT or those that use SSP (Spatial Smoothing Preprocessing) cannot be compensated. These methods require sub-array antennas with identical characteristics. However, the sub-array antenna is usually selected from a single array antenna; hence, mutual coupling also affects these algorithms. In this case, fine adjustment of the element interval can reduce the DOA estimation error. This method has a limitation, that is, it is only applicable to linear array antennas with half-wavelength intervals.

Figure 4.11 (a) shows the estimation error in the ESPRIT algorithm without adjusting the element interval. Figure 4.11 (b) and (c) show the estimation error in the ESPRIT algorithm by adjusting the element interval. The element interval was adjusted to $0.5\lambda + \alpha$; α is varied to $\pm 1 \times 10^{-2}\lambda$, $\pm 2 \times 10^{-2}\lambda$, and $\pm 3 \times 10^{-2}\lambda$. The value $1 \times 10^{-2}\lambda$ corresponds to 0.35 mm at 8.45 GHz. The minimum limit to adjust the element position is approximately 0.1 mm in a handmade experimental setup. In the case of a large interval, the error is less than 2° for $|\theta| < 60°$, and it increases rapidly for $|\theta| > 60°$. In the case of large arrival angles, the estimation error becomes larger than the DOA angle. On the other hand, the error for an arrival angle when $|\theta| < 60°$ is very small even if element position error exists. In the case of a small element interval, as shown in Figure 4.11 (b), the error is less than 2° for $|\theta| < 30°$, and it increases gradually for larger arrival angles. It should be noted that we can obtain accurate DOA estimation results for $|\theta| < 30°$ even if mutual coupling and element positioning error exist. This phenomenon is valid for a large number of array elements and serves as a useful criterion from a practical point of view.

In order to obtain a simple error compensation method, the optimum element position that minimizes the estimation errors is examined. Figure 4.12 shows the estimation error rate for $|\theta| < 60°$ and $|\theta| < 90°$ by varying the element position. The error rate is the summation of estimation errors at each arrival angle wherein each value is normalized by the maximum estimation error of 90°. The inaccuracy of the element interval α was varied from $-5 \times 10^{-2}\lambda$ to $+5 \times 10^{-2}\lambda$ in intervals of $0.5 \times 10^{-2}\lambda$. In the

case of $|\theta| < 90°$, the rate is minimized at an element spacing of 0.5λ with no positioning error. However, the error rate for $|\theta| < 60°$ is minimized at an element spacing of $\alpha = +2 \times 10^{-2}\lambda$. On the basis of this result, the total error can be suppressed by maintaining a slightly large element interval for the arrival angle of $|\theta| < 60°$.

Figure 4.13 shows the error in the experimental measurements using the DBF array antenna at 8.45 GHz. The construction of the experimental environment is shown in Figure 2.7. The array antenna has intervals of less than $1 \times 10^{-2}\lambda$. The estimation error in the case of a large interval is smaller than that in case of a small interval within ± 60°, and thereafter it increases rapidly. The measurement result is similar to the simulation result, as shown in Figure 4.11.

4.3.2 Low Coupling Array Antenna System

In order to achieve the specification mentioned in section 3.2.4, a low-coupling patch array antenna is designed. Figure 4.14 shows the configuration of an element of the array antenna. The mutual coupling of this antenna is suppressed by a box-shaped metallic wall around the microstrip patch. The wall is connected to the ground plane of the microstrip antenna. These antenna elements are arrayed at half-wavelength intervals (Figure 4.15). The sizes of the walls L_x, L_y, h_x, and h_y were optimized by computer simulation in order to achieve mutual coupling of –30 dB between neighboring elements. The optimized parameters are $L_x = 0.4\lambda$, $L_y = 0.5\lambda$, $h_x = 0.25\lambda$, and $h_y = 0.2\lambda$ in order to obtain a maximum mutual coupling of –33 dB at 5 GHz in the experiment. Figure 4.16 shows the S parameters between #2 and #3 of the array antenna. The characteristics were identical and a mutual coupling of –33 dB was achieved.

Using the array antenna with a box-shaped metallic wall, the estimation errors of ESPRIT are evaluated using a 4-channel DBF array antenna at 5 GHz in an

anechoic chamber. Figure 2.7 shows the measurement setup. A transmission source is installed in front of the array and the array antenna is set on a rotator in order to change the DOA. The receiver is calibrated with $\theta = 0°$ and the array antenna patterns are not calibrated. The array antenna consists of a normal microstrip patch antenna (a) and a box-shaped metallic wall (b). The relation between the DOA and the estimation error is shown in Figure 4.17. The maximum value of the estimation error with (b) is 0.4° for $\theta < 25°$, and it is reduced by 0.8° with (a); however, the error for $25° < \theta < 60°$ is not reduced because the half-power width of the pattern is approximately 50° (Figure 4.18). Based on the above, it can be concluded that a low-coupling microstrip patch array antenna with a box-shaped metallic wall is effective in reducing the estimation error in the ESPRIT method.

4.3.3 Increase in the Number of Elements by Rotating the Array Antenna

In this section, we describe the effects of the increase in the number of elements by rotating the array antenna. We use the DOA estimation by the MUSIC algorithm in the anechoic chamber as shown in Figure 2.7. Two transmitting antennas (each has a different antenna gain) were installed at –10° and 20° in the direction of the receiver of the DBF array antenna. We rotate the antenna element by 180° around the center element and increase the number of antenna elements virtually, as shown in Figure 4.19. This rotation is achieved by using the rotator that provides a precise angle. The phase is adjusted based on the center element of rotation. Therefore, we can obtain a 7-element low-cost DBF array antenna from the 4-element antenna. Figure 4.20 shows the DOA (two wave sources) estimation result obtained using the 7-element DBF array antenna. This result indicates that the 7 elements can be estimated in a manner similar to that used to obtain 4 elements. In addition, it improves the resolution of DOA estimation by a greater extent than that obtained using 4 elements. As indicated by this result, the

DOA (three wave sources) can be estimated by using the 7-element DBF array antenna. Therefore, by increasing the number of elements, we can improve the resolution of DOA estimation using this DBF array antenna. Thus, we can estimate the DOA of several waves by increasing the number of elements in this system.

4.4 Conclusion

In this chapter, we proposed a calibration method for suppressing the error factors examined in Chapter 2 and. The steering vector compensation method is the most basic calibration method. The measurements were performed in the anechoic chamber and spline interpolation was effective up to a 20° interval. Coupling calibration was performed using a fixed calibration antenna that can be calibrated during operation. At an optimum condition, the estimation error was suppressed within 1°. The correlation matrix estimation method for the transmitting array antenna was demonstrated experimentally in the anechoic chamber. The array antenna element pattern changes due to several error factors; however, by optimum adjustment of the element interval, mutual coupling, and the number of elements, a high-precision array antenna system with reduced errors can be obtained.

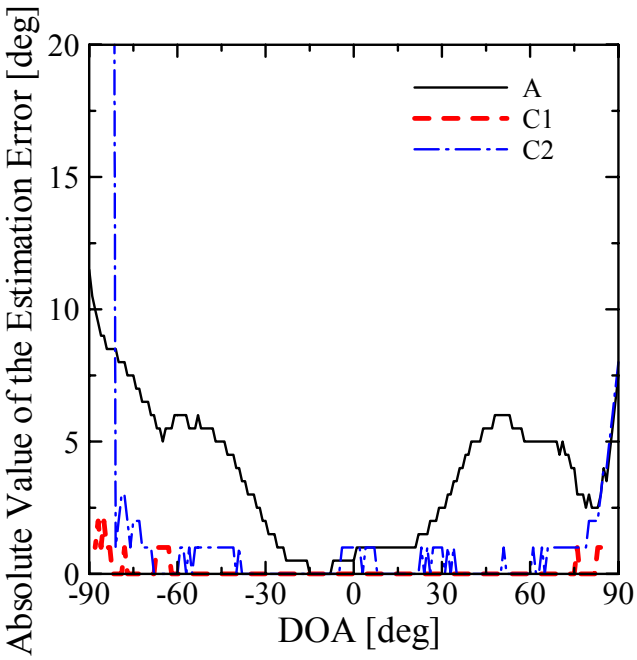

(a) 2.6 GHz

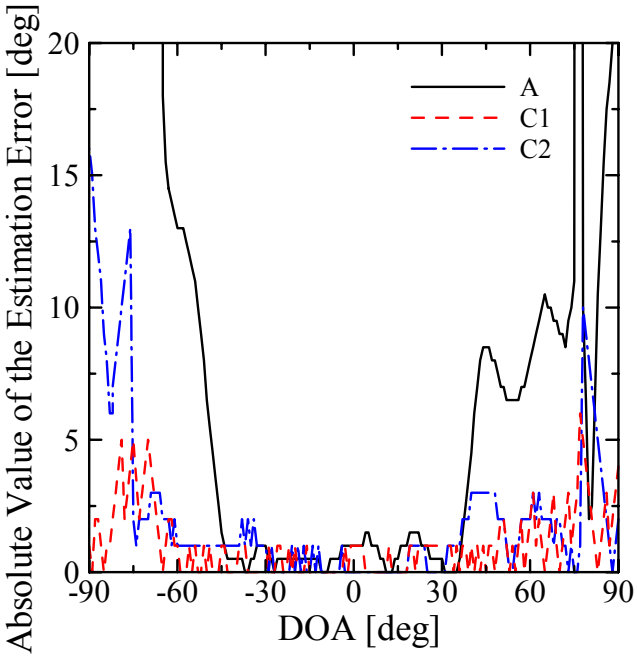

(b) 8.45 GHz

Figure 4.1: Estimation error (before and after compensation) (measurement).

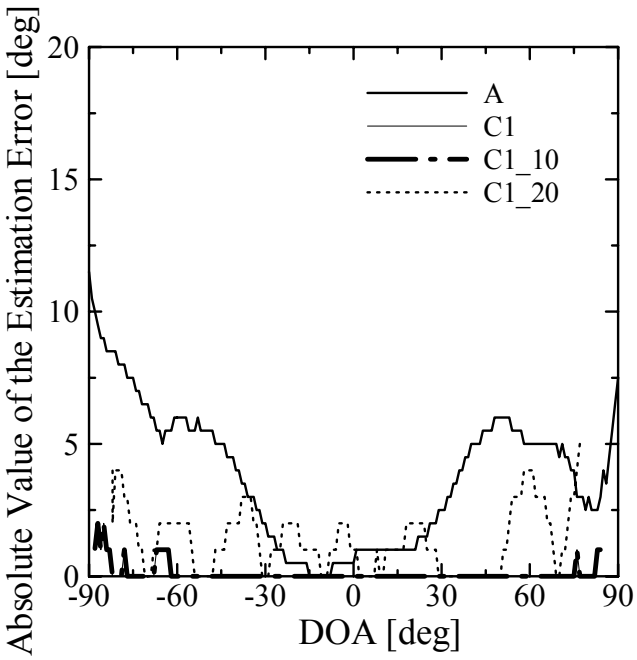

(a) 2.6 GHz

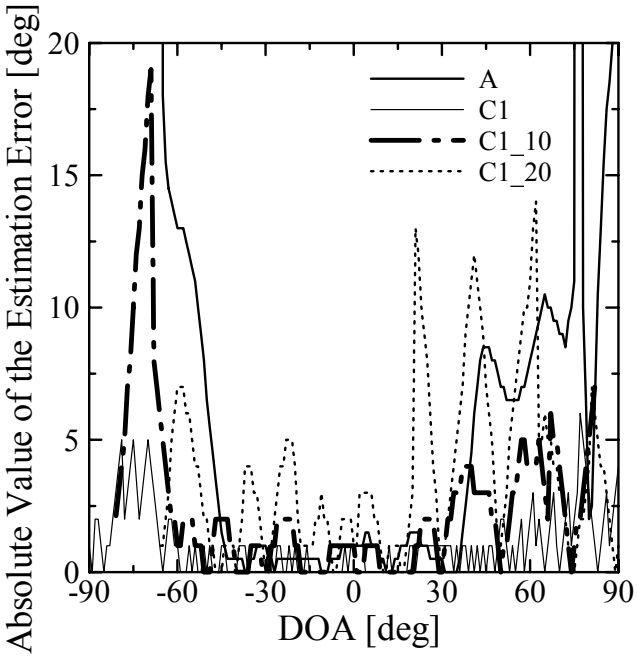

(b) 8.45 GHz

Figure 4.2: Estimation error (interpolation of the mode vector) (measurement).

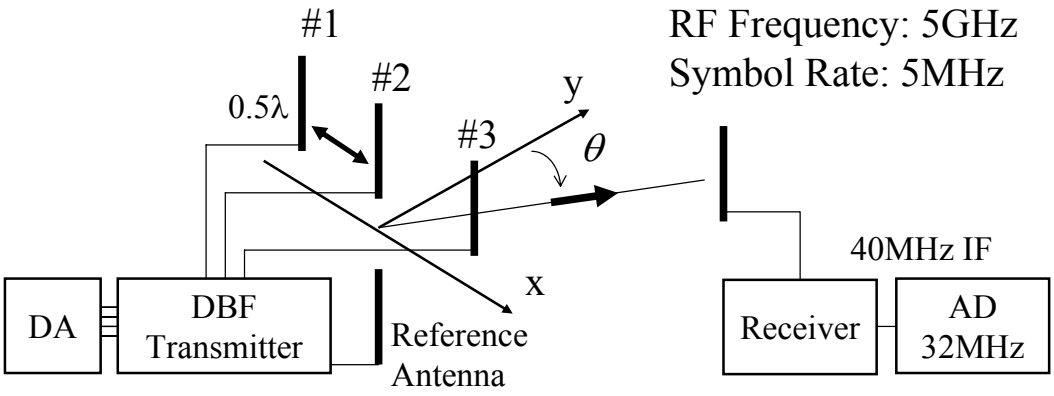

Figure 4.3: Calibration system of the transmitting array antenna.

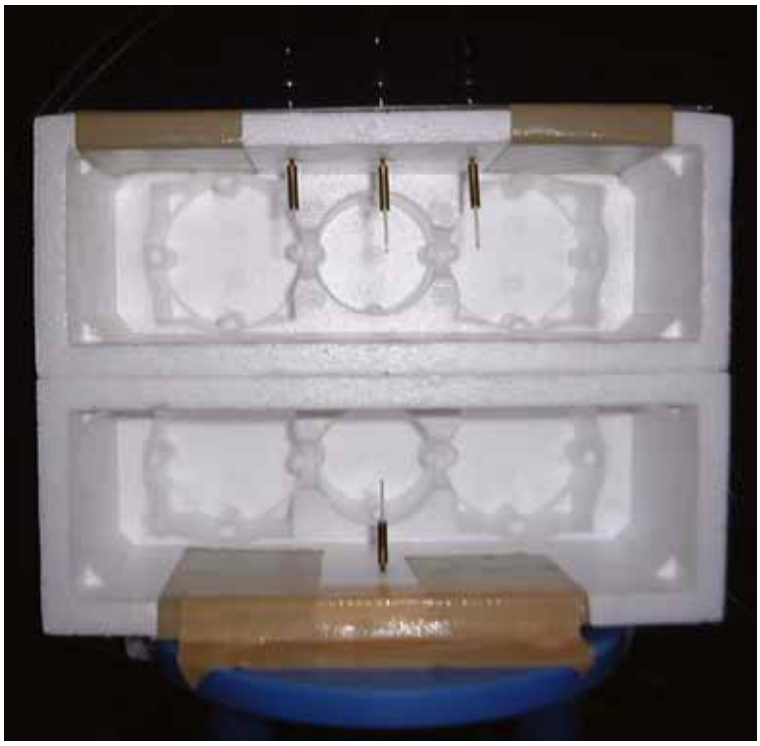

Figure 4.4: Transmitting array antenna.

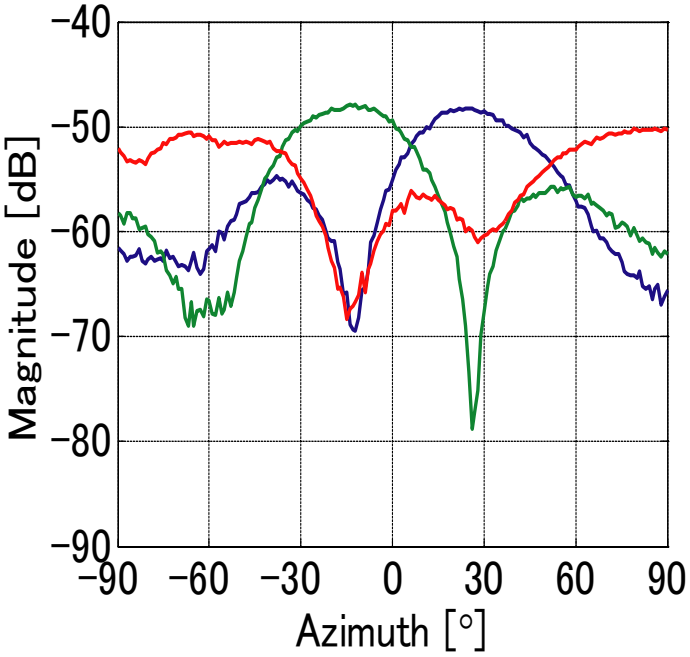

(a) Synthesized pattern

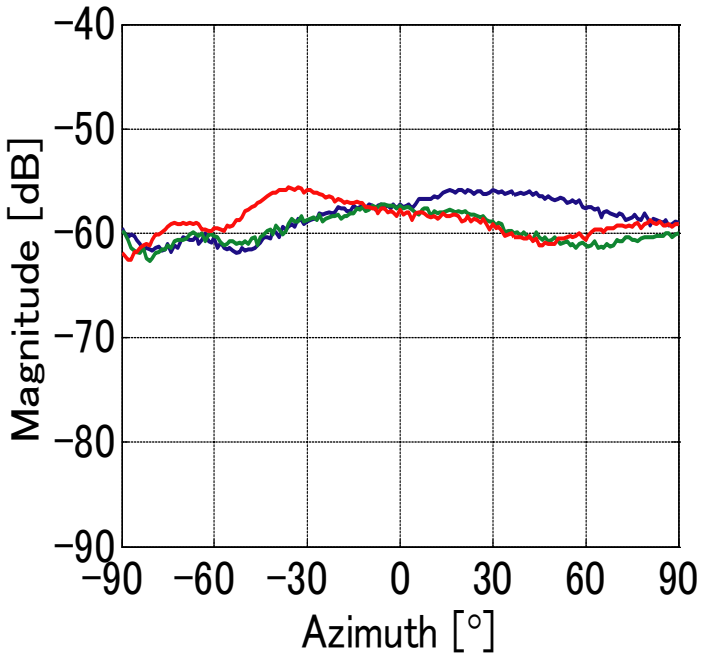

(b) Amplitude pattern of each element

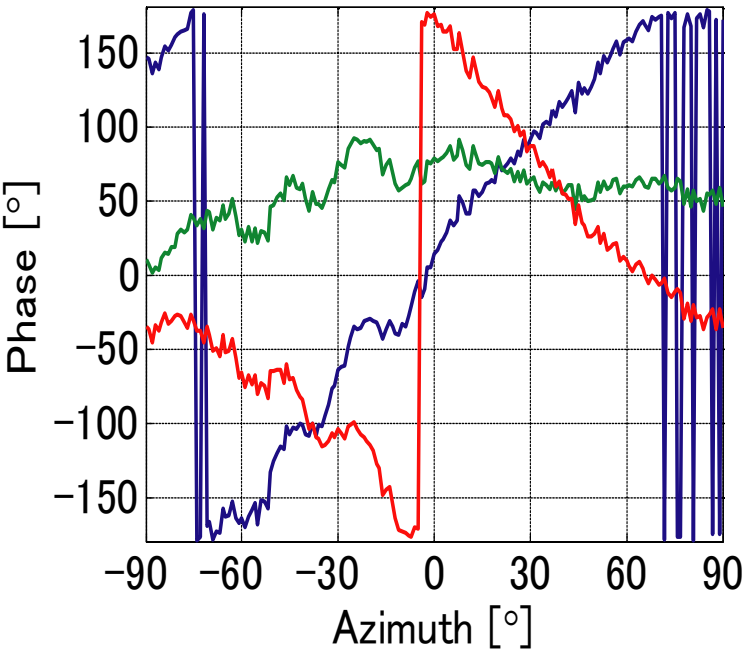

(c) Phase pattern of each element

Figure 4.5: Patterns before calibration (measurement).

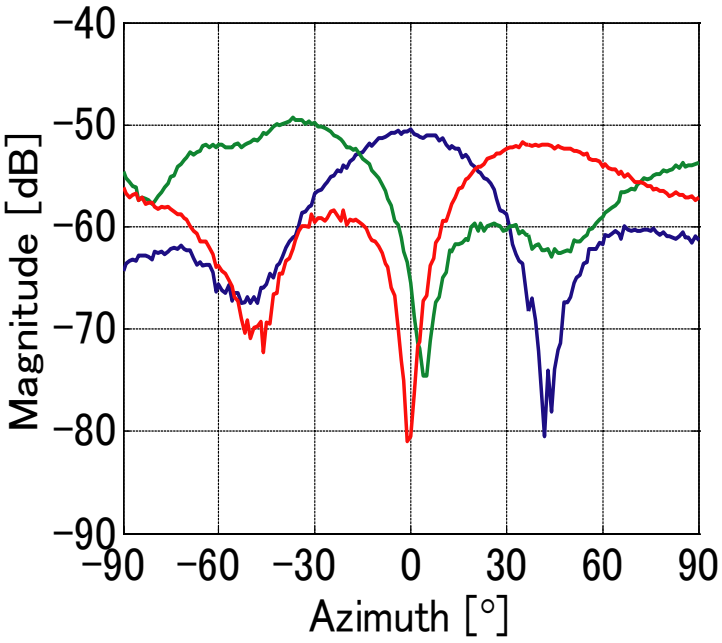

(a) Synthesized pattern

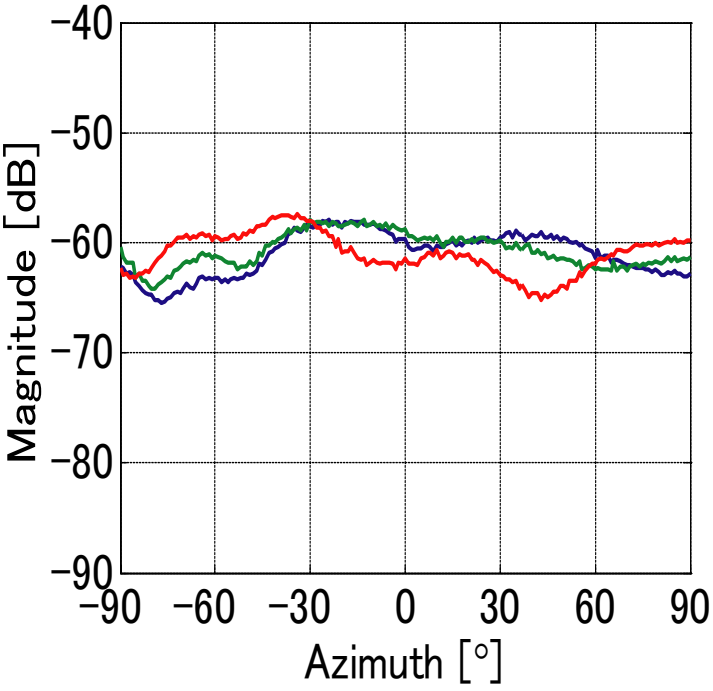

(b) Amplitude pattern of each element

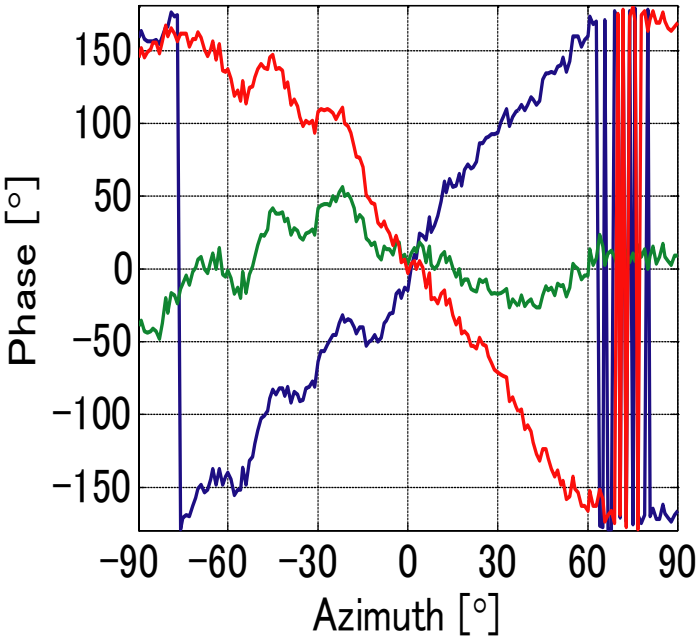

(c) Phase pattern of each element

Figure 4.6: Patterns after calibration (measurement).

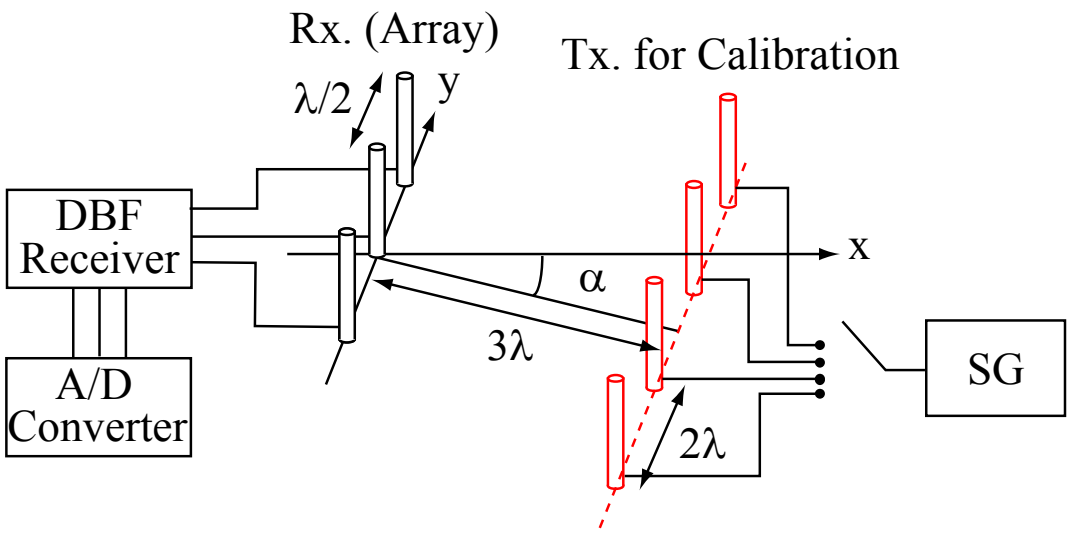

Figure 4.7: Coupling calibration system using a fixed calibration antenna.

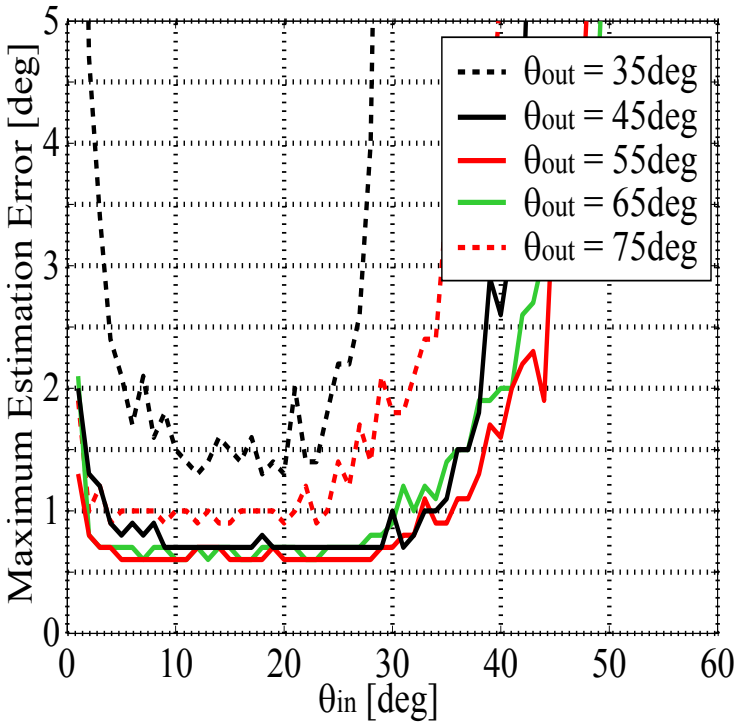

Figure 4.8: Estimation error by varying the fixed calibration antenna element positions (simulation).

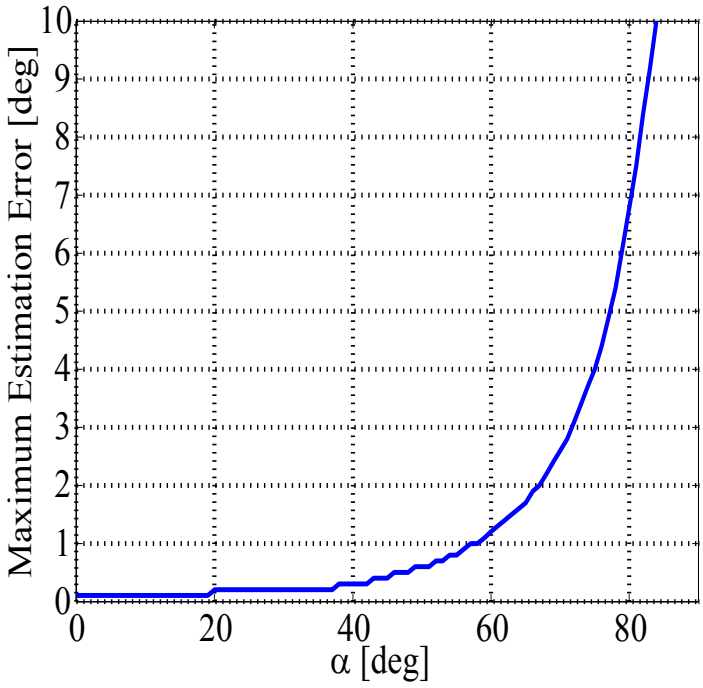

Figure 4.9: Estimation error by varying the elevation of the array antenna (simulation).

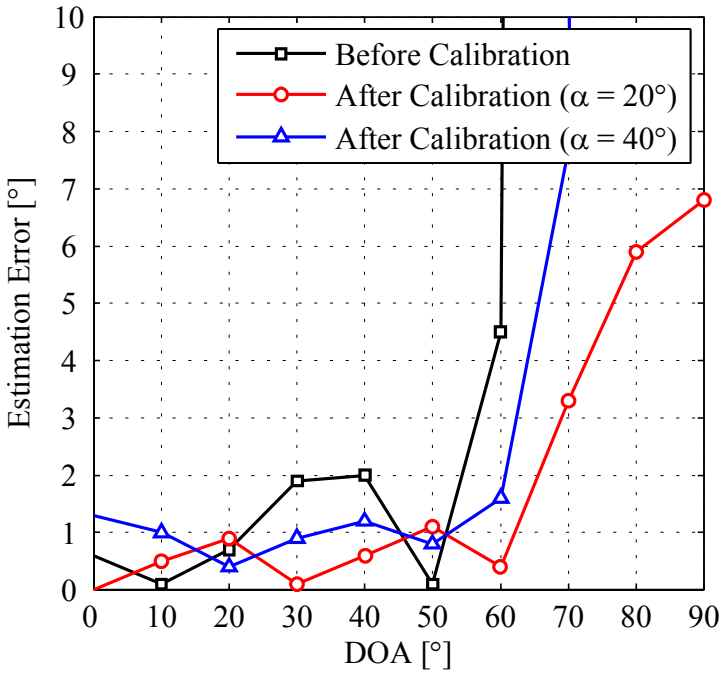

Figure 4.10: Estimation error (measurement).

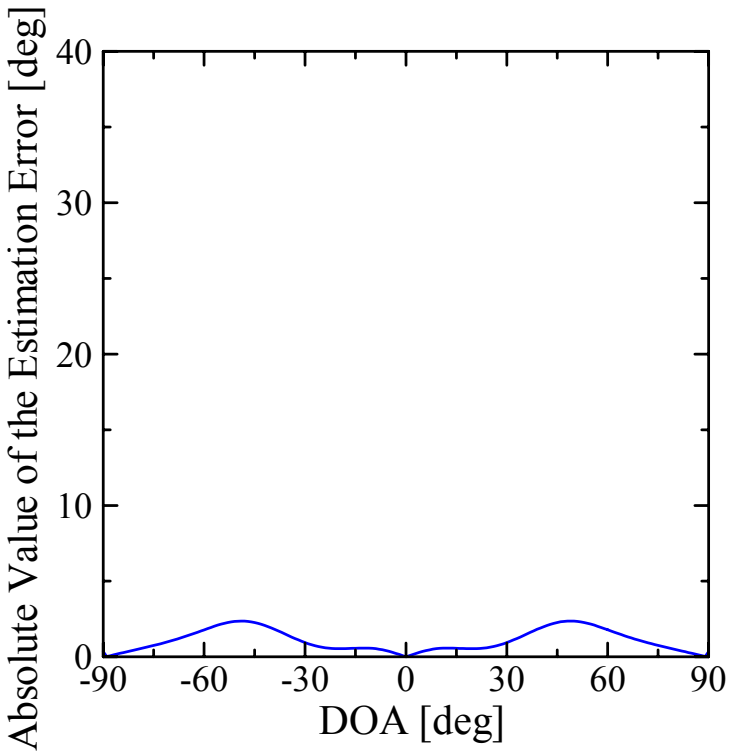

(a) Element interval of 0.5λ

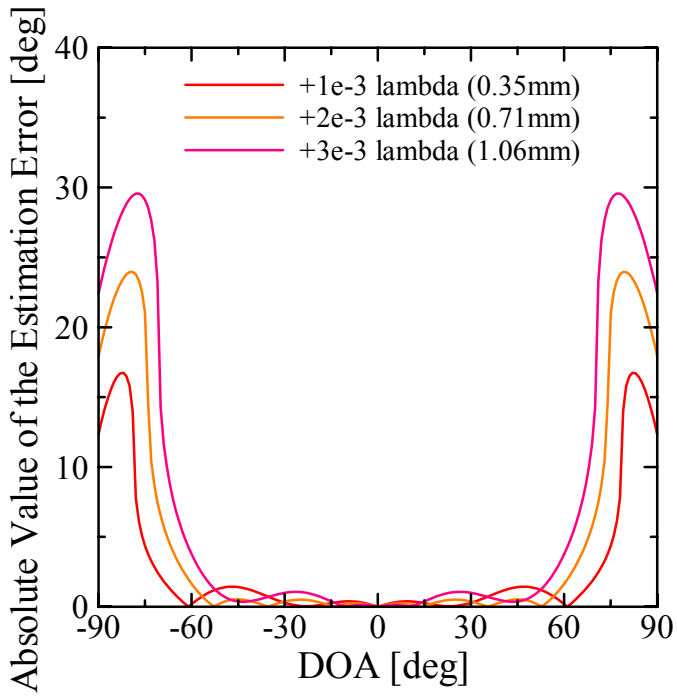

(b) Element interval of 0.5λ + α

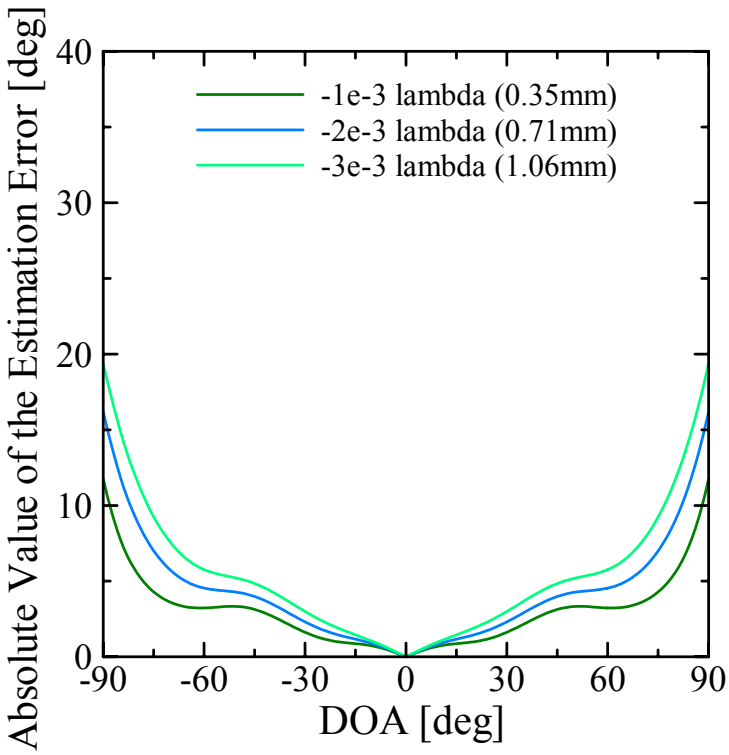

(c) Element interval of 0.5λ – α

Figure 4.11: Estimation error with mutual coupling (simulation).

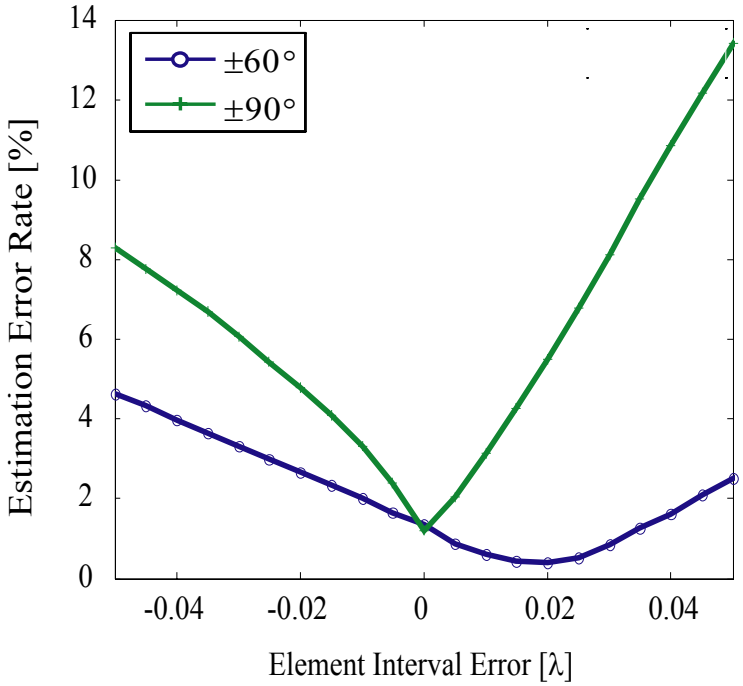

Figure 4.12: Estimation error rate (simulation).

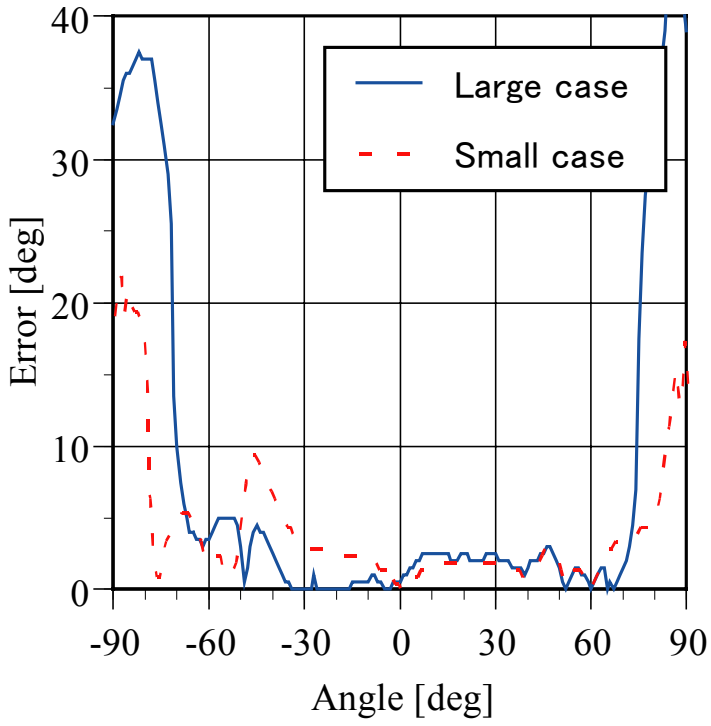

Figure 4.13: Estimation error (measurement).

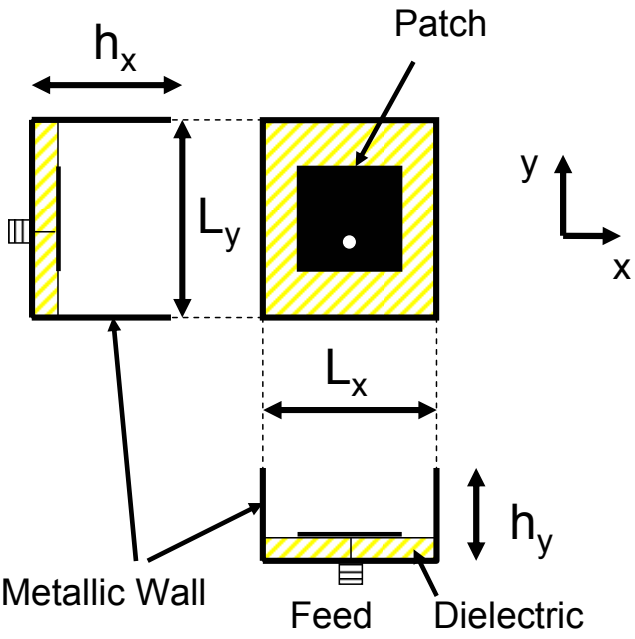

Figure 4.14: Microstrip antenna with a box-shaped metallic wall.

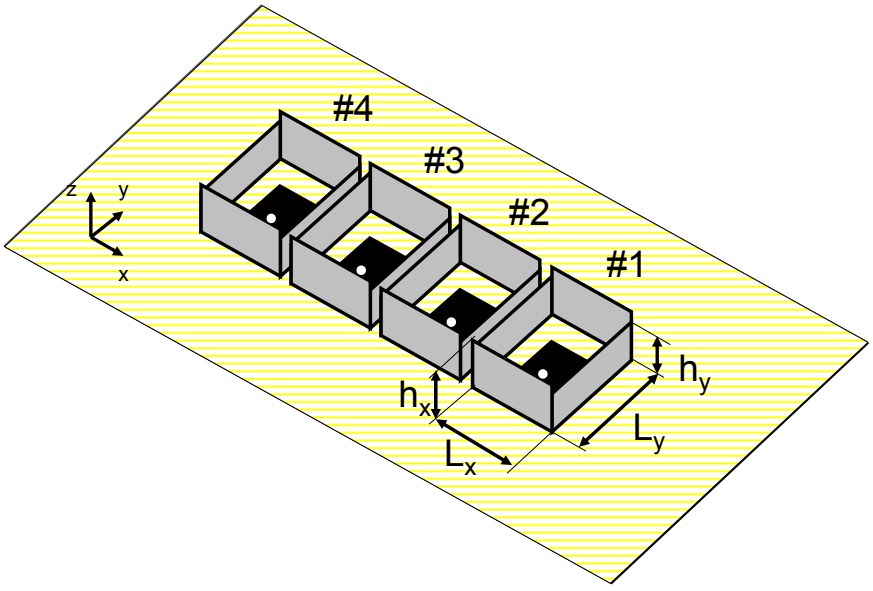

Figure 4.15: 4-element linear array antenna with half-wavelength intervals.

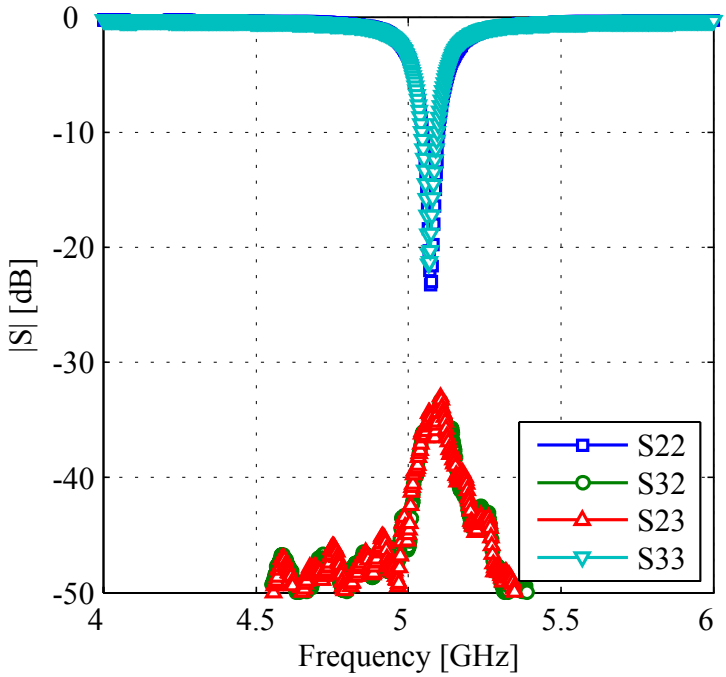

Figure 4.16: S parameters between #2 and #3.

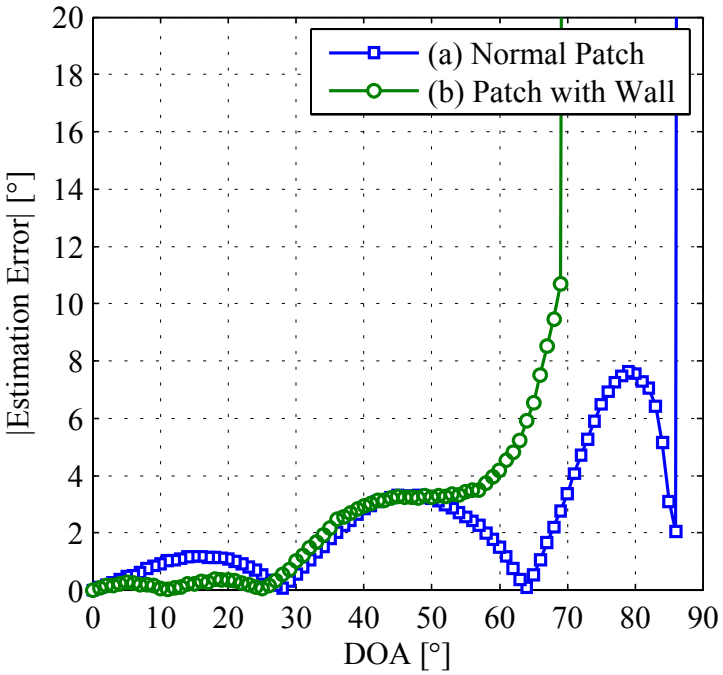

Figure 4.17: Estimation error (measurement).

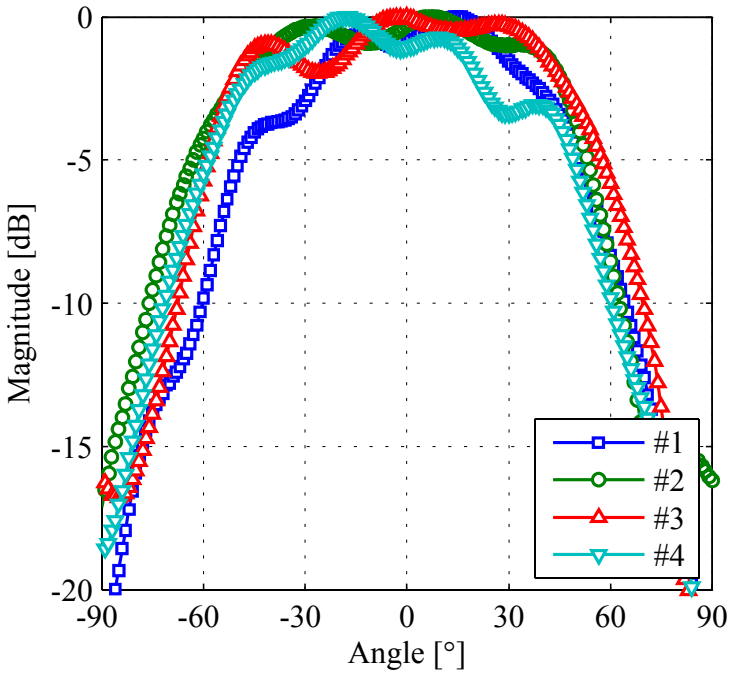

Figure 4.18: Element pattern (x-z plane) (measurement).

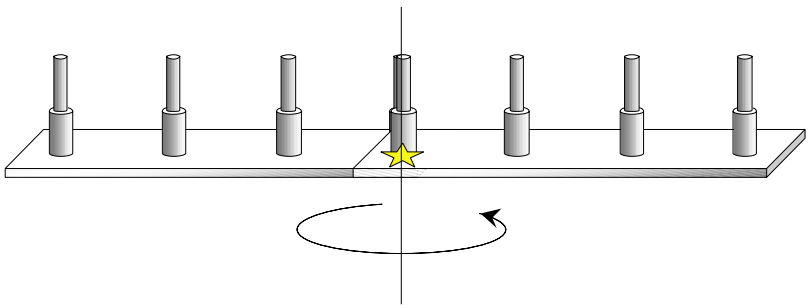

Figure 4.19: Rotation of the array antenna.

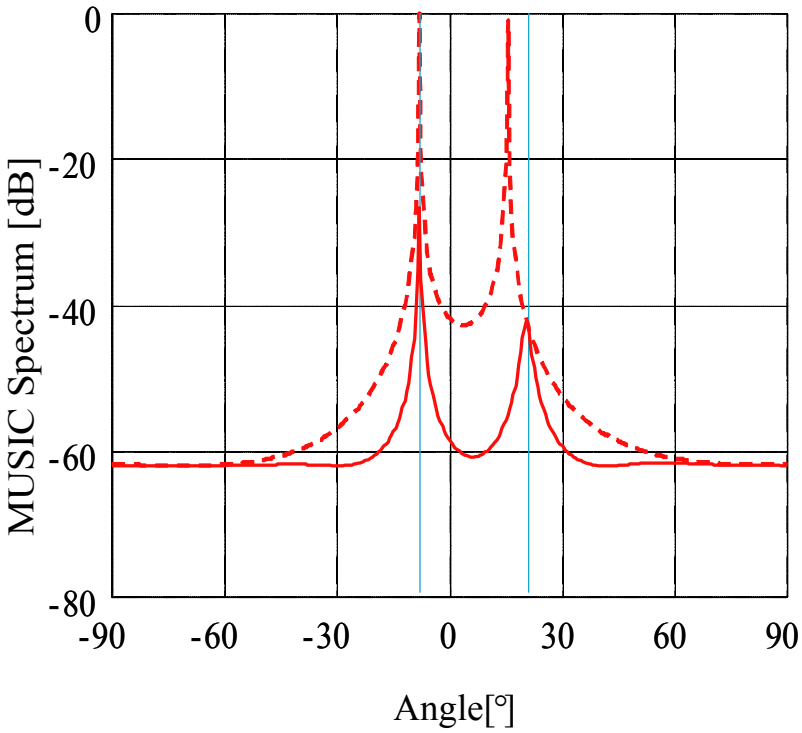

Figure 4.20: Estimation error (measurement).

Chapter 5

Conclusion

This dissertation described the attempt to achieve a high-precision array antenna system for the adaptive antenna in mobile communication.

In chapter 2, we formulated the array antenna and DOA estimation and explained prototype array antenna systems. An evaluation method using a rotating array antenna was proposed. We analyzed the error factor based on experiments conducted in the anechoic chamber. We evaluated the array antenna system using DOA estimation, and on the basis of this evaluation, we clarified the problems related with the hardware and propagation environment. The DOA estimation error is large due to errors from inaccuracies in the array element interval and mutual coupling. These errors are not independent, and they vary with the antenna structure and machining accuracy. These errors were examined in detail in the following chapters.

In chapter 3, we conducted a detailed examination of the errors due to inaccuracy in array element positions, mutual coupling of elements, and plane wave approximation wherein the distance between transmitting and receiving antennas is small. First we formulated the array antenna that takes into account the effects of the antenna element pattern and used the moment method to quantitatively and statistically analyze mutual coupling and the DOA estimation error. When the inaccuracy of the array element position at a radius of $0.1\times10^{-2}\lambda$ is within 99.7%, the DOA estimation

error decreases to below 0.5° for a DOA that is less than 60°, and dispersion was negligible. The value $0.1 \times 10^{-2}\lambda$ corresponds to 35.5 μm and 112 μm at 8.45 GHz and 2.665 GHz, respectively. Next, changing simulation was carried out by varying the extent of mutual coupling. The estimation error is minimized when the mutual coupling between neighboring elements is –30 dB and the dispersion of the amplitude and phase of the element pattern is within 1 dB and 5°, respectively. The influence of the distance between the transmitting and receiving array antennas is less than 0.1° when the distance is greater than approximately 10λ. The distance of 10λ corresponds to 35.5 mm and 112 mm at 8.45 GHz and 2.665 GHz, respectively.

In chapter 4, we proposed a calibration method for suppressing the error factors examined in Chapter 2. The steering vector compensation method is the most basic calibration method. The measurements were performed in the anechoic chamber and spline interpolation was effective up to a 20° interval. Coupling calibration was performed using a fixed calibration antenna that can be calibrated during operation. At an optimum condition, the estimation error was suppressed within 1°. The correlation matrix estimation method for the transmitting array antenna was demonstrated experimentally in the anechoic chamber. The array antenna element pattern changes due to several error factors; however, by optimum adjustment of the element interval, mutual coupling, and the number of elements, a high-precision array antenna system with reduced errors can be obtained.

Inaccuracy of array element position and mutual coupling of elements influence each other and cause a DOA estimation error or adaptive null steering in antenna element pattern. A high-precision array antenna system can be achieved through optimal adjustment of these factors.

Appendix A

Signal Discrimination Method Based on the Estimation of Signal Correlation using an Array Antenna

A.1 Introduction

At present, various algorithms for array antenna signal processing are proposed; however, the characteristics of these algorithms are often altered by propagation environments [20]. A solution to this problem includes estimating the characteristics of the propagation environment in real time and the switching algorithm based on the data obtained. Therefore, we focused on real-time estimation methods of propagation environments. Methods [21], [22] that have been extensively studied can estimate the characteristics of propagation environments with high accuracy and are suitable for propagation model analysis. However, they are inappropriate for real-time estimation because they require tremendous computational effort and special measurements such as frequency sweep and synchronization of transmitter and receiver. There are few studies on real-time estimation methods for propagation environments [23]. FFT-MUSIC [24] is a high-speed estimation method for propagation environments that uses direction of arrival (DOA), delay time, and power of signals and the

implementation of the equipment and facilities for this method has been reported [25]. This method works on the principle of converting the received time-domain PN code to frequency domain by fast Fourier transform, estimating the delay time by MUSIC method [26], and estimating the DOA and power with a general retrogression sequence operation. However, the knowledge of PN code is essential at the receiving end.

In this appendix, we propose a real-time signal discrimination method based on the estimation of signal correlation using an array antenna. This method is a combination of common DOA estimation by eigenvalue analysis, such as MUSIC or ESPRIT, and signal correlation estimation. Although delay-time estimation has a limitation, this method can estimate the characteristics of the propagation environment without any special measurements, provided the transmitted signal is digitally modulated with a random source similar to the PN code. Therefore, this method is suitable for real-time estimation of propagation environment characteristics. Section 2 describes the principle of the proposed method and a comparison with the FFT-MUSIC method using simulations. Section 3 presents the results of the experiments in an anechoic chamber and an indoor environment, and it establishes the validity of the proposed method.

A.2 Signal Discrimination Method

In this section, the principle of the proposed method is described. Figure A.1 shows the system and the assumed environment. The transmitted signals are digitally modulated with a random source and band limited with a root-Nyquist filter before transmission. At the receiving end, the signal received with the array antenna is band limited with a root-Nyquist filter in terms of the transmitting end and is given as a base-band signal. An IF signal can also be used for the estimation; however, only

base-band processing is described in this section. At the receiving end, only the information of the transmitting Nyquist filter is required, whereas information, such as transmitting data or synchronization timing is not required. Figure A.2 shows an overview of the proposed method. The estimation is performed in 3 steps: DOA estimation, signal correlation matrix estimation, and delay time and power estimation. Super-resolution estimation methods such as MUSIC, ESPRIT, and SSP (Spatial Smoothing Preprocessing) that employ eigenvalue analysis are used for the DOA estimation.

The signal correlation matrix is estimated by a general retrogression sequence operation and the derived delay time and power of signals. In delay time estimation, the relative delay value for the symbol rate can be estimated only when more than 2 waves originate from the same user. When the delay time is greater than one symbol, the signal is estimated as signal from another user. With accurate DOA estimation, the signal correlation matrix can be estimated by general retrogression sequence operation with the following equation:

$$\mathbf{S} = \left(\mathbf{A}^H \mathbf{A}\right)^{-1} \mathbf{A}^H \left(\mathbf{R}_{xx} - \sigma^2 \mathbf{I}\right) \mathbf{A} \left(\mathbf{A}^H \mathbf{A}\right)^{-1} \tag{A.1}$$

The diagonal elements of $\boldsymbol{S}$ represent the power of each signal and the non-diagonal elements indicate the covariance. This operation is commonly used for the estimation of signal power by the MUSIC method. Normalizing $\boldsymbol{S}$ and defining it as $\boldsymbol{r}$, the (i,j) elements are given as follows:

$$r_{i,j} = \frac{S_{i,j}}{\sqrt{S_{i,i} \cdot S_{j,j}}} \tag{A.2}$$

By defining the band-limited random sequence of sufficient length, which is obtained

from the Nyquist filter with an impulse response of $h(t)$ as $f(t)$ on the basis of the Wiener-Khintchine theorem, the auto-correlation function of the received signal $R(\tau)$ is equal to the inverse Fourier transform of the received signal spectrum $h(\tau)$.

$$\begin{aligned} R(\tau) &= \int_{-\infty}^{\infty} f(t) \cdot f(t-\tau) dt \\ &= h(\tau) \end{aligned} \tag{A.3}$$

This determines the relation between the delay and signal correlation of the arrived signal. By defining the inverse function of h as h^{-1} within the range of a one-one relation, the delay τ can be estimated from the signal correlation by the following equation:

$$\tau = h^{-1}\left(r_{i,j}\right) \tag{A.4}$$

However, when the delay time is greater than that of one symbol, the relation is overspecified and the correlation varies in the vicinity of 0. The proposed method estimates the signal from another user, provided the information of the transmitting signal is not used. The computational effort of the proposed method increases slightly due to delay estimation because it is only possible to achieve the look-up table of h^{-1}. Furthermore, the total computational effort of the proposed method is considerably less than that required for a 2-dimensional estimation of direction and time delay.

The FFT-MUSIC method performs FFT processing of a time-domain signal and estimates the delay time by the MUSIC method using the data of the frequency series and then estimates the DOA. Further, it can perform the same estimation as this technique in an environment with a signal from the same source. Figure A.4 shows the comparison of the calculation time ratios on the basis of the calculation time of FFT-MUSIC with 4 elements. Figure A.5 shows the estimation error of the simulation in the case of 2 wave sources, 8 elements, and 10 dB SNR. The first wave source is fixed

at −10° and the second source is varied from −5° to 30° for every 5°. Their delay time is 0 ns and 200 ns (1 symbol cycle), respectively. It is verified that the proposed method is excellent in terms of calculation accuracy; however, the number of calculations vary depending on the number of elements.

A.3 Measurement in an Anechoic Chamber and Indoor Environment

The experimental specifications of the system are listed in Table A.1. The RF signal received from the array antenna passes through two steps of frequency conversion and is changed to a 40 MHz IF signal for each element. The signals are sampled by 12-bit 32 MHz AD converters, converted to base-band signals, and processed by the proposed method with off-line processing using a PC. Before performing the measurement, the array antenna and receiver are calibrated with a CW signal from a transmitting antenna installed in front of the receiving array by adjusting the amplitude and phase through an adjustment circuit of the receiver in the anechoic chamber, assuming that all waves are plane waves.

Figure A.6 shows the experimental setup in the anechoic chamber. Two transmitting antennas, with directions of –25° and 25°, respectively, are set in front of the receiving array antenna. The delay of the left transmitting antenna is fixed, while that of the right antenna is varied from 0 to 2 symbols. The relation between delay and correlation coefficient obtained both theoretically and from the measurement is shown in Figure A.7. Here, the Nyquist filter has cosine roll-off characteristics ($\alpha = 0.5$). The theoretical and measured values are largely in good agreement and they confirm that delay under 0.7 symbol can be easily obtained from a self-correlation function with $r_{i,j}$

over 0.4. Figure A.8 shows the estimation result of the proposed method. The delay is varied for every 0.2 symbol. The delay from 0 to 1 symbol is estimated accurately within 0.2 symbol.

Next, the measurement in an indoor environment is carried out using the same system in an anechoic chamber. Figure A.9 shows the experimental setup in an indoor environment. One transmitting antenna is set at a distance of 3 m from the receiving array. The left wall consists of a glass door with a metal sash and the right wall is made of concrete with an irregular surface. The transmitting power is −20 dBm. Figure A.10 shows the estimation result of the proposed method. Two signals arrive from −35° and 10° and the slight delay is measured from the result. With respect to the position of the antenna and wall, the left signal is reflected from the sash of the glass door and the right signal is a direct wave. Figure A.9 shows the difference in the distance traveled by the two waves to be 1.4 m (0.02 symbol); hence, the delay is estimated accurately within 0.2 symbol.

A.4 Conclusion

In this section, we proposed a real-time signal discrimination method based on the estimation of signal correlation using an array antenna. This method is a combination of common DOA estimation by eigenvalue analysis and signal correlation estimation. This method is suitable for real-time estimation of propagation environment characteristics. A comparison with the FFT-MUSIC method through simulations and the results of experiments in an anechoic chamber and in an indoor environment showed the validity of the proposed method. The delay from 0 to 1 symbol was estimated accurately within 0.2 symbol during the measurements. Future studies of the proposed method could evaluate a case in which there are more than 2 users, an environment with angler

spread, and wherein the number of array elements is less than the number of waves.

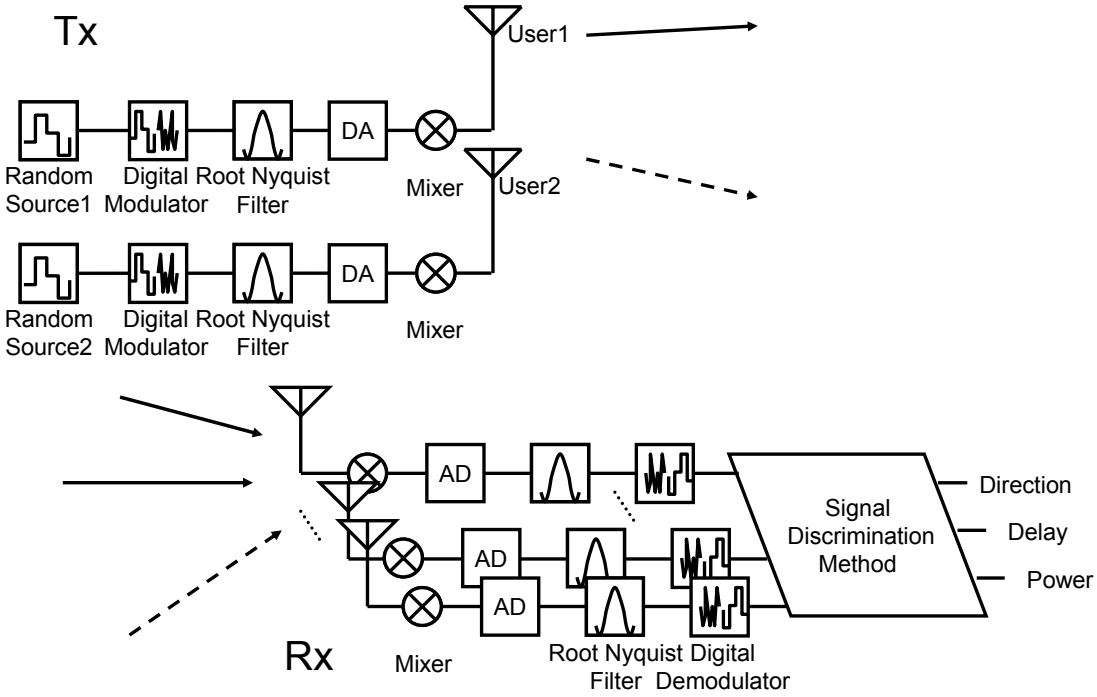

Figure A.1: System and environment.

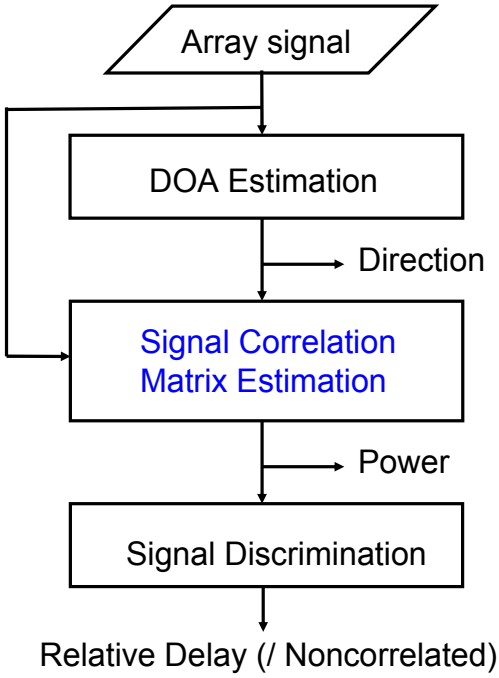

Figure A.2: Overview of the proposed method.

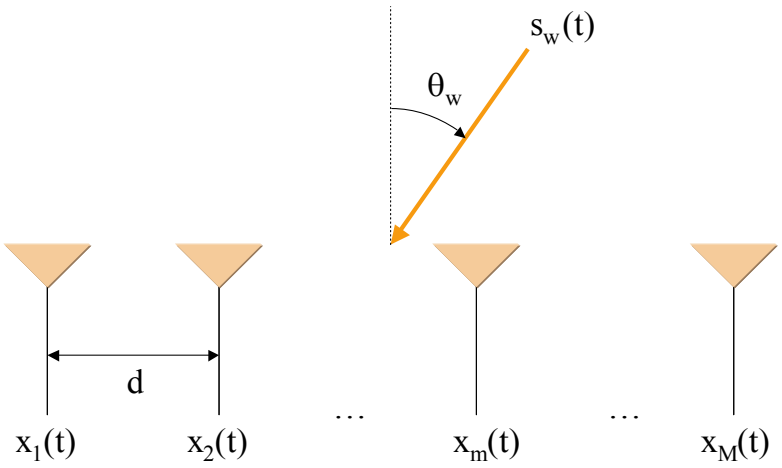

Figure A.3: Array Antenna.

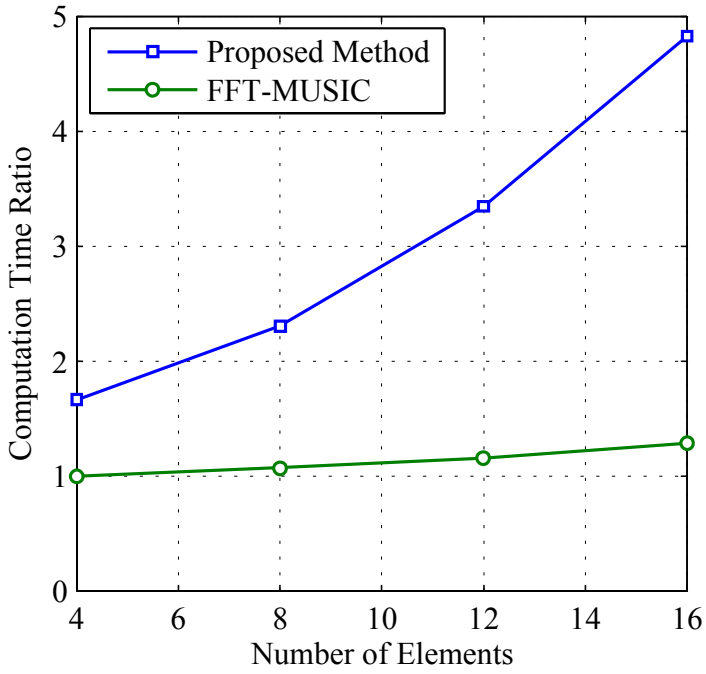

Figure A.4: Comparison of calculation time (simulation).

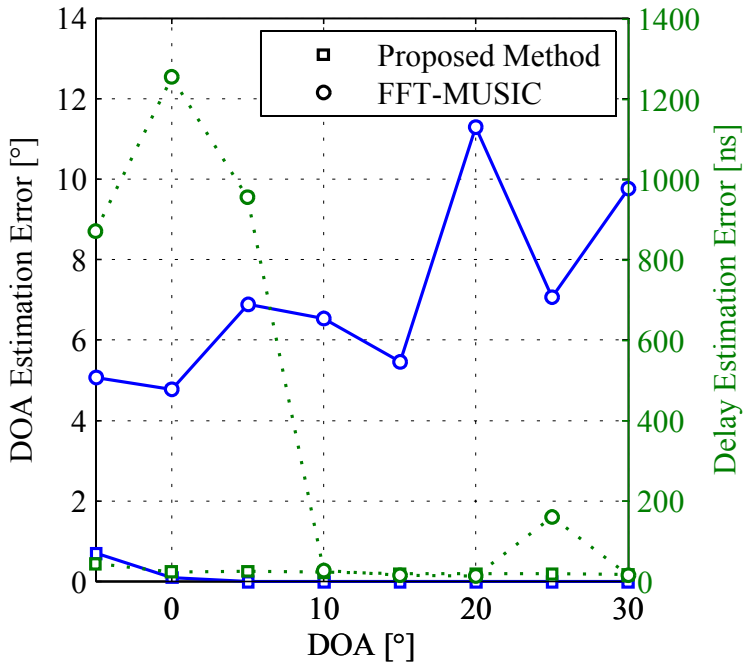

Figure A.5: Estimation error (Black: DOA, Gray: Delay) (simulation).

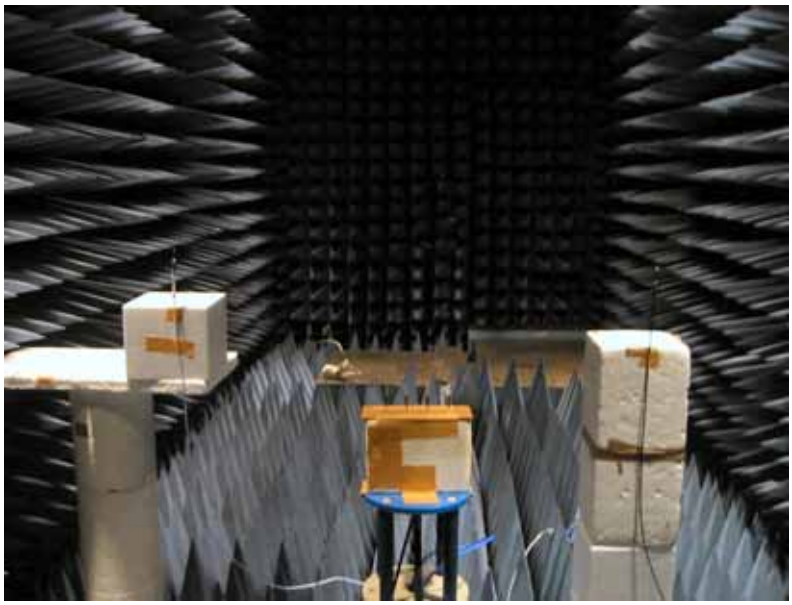

(a) Experimental setup

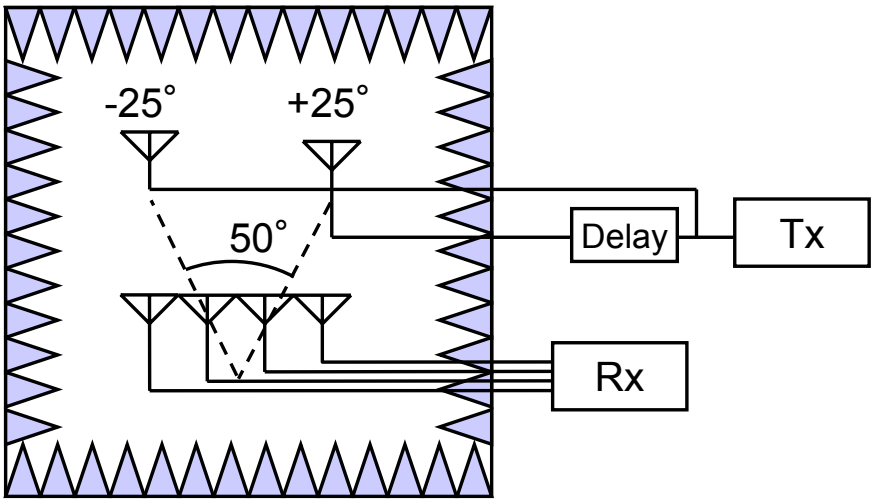

(b) Transmitting antenna and receiver array position

Figure A.6: Measurement in an anechoic chamber.

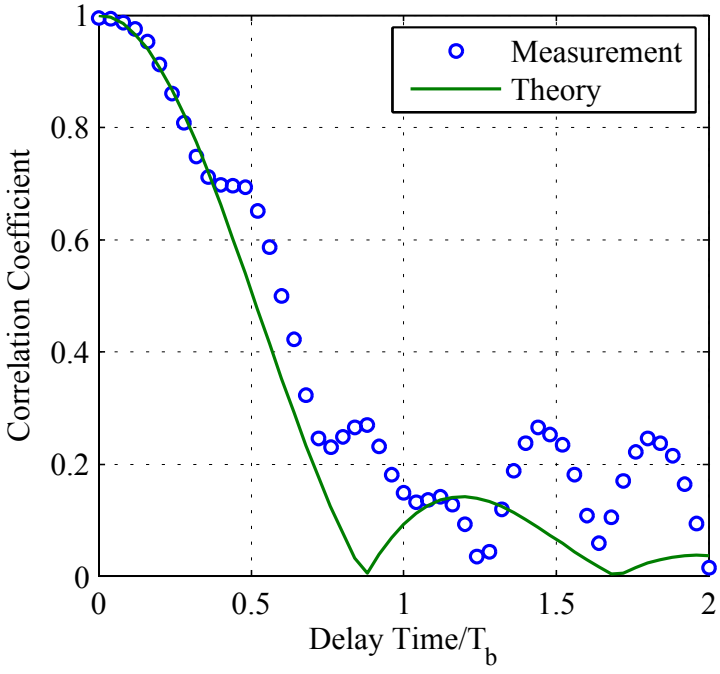

Figure A.7: Relation between delay and correlation coefficient.

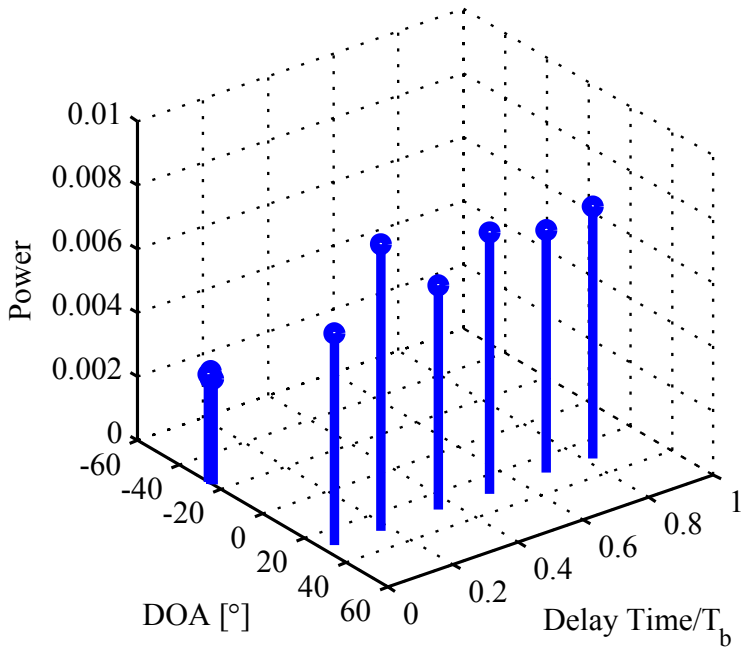

(a) Delay from 0 to 1 symbol (every 0.2 symbol)

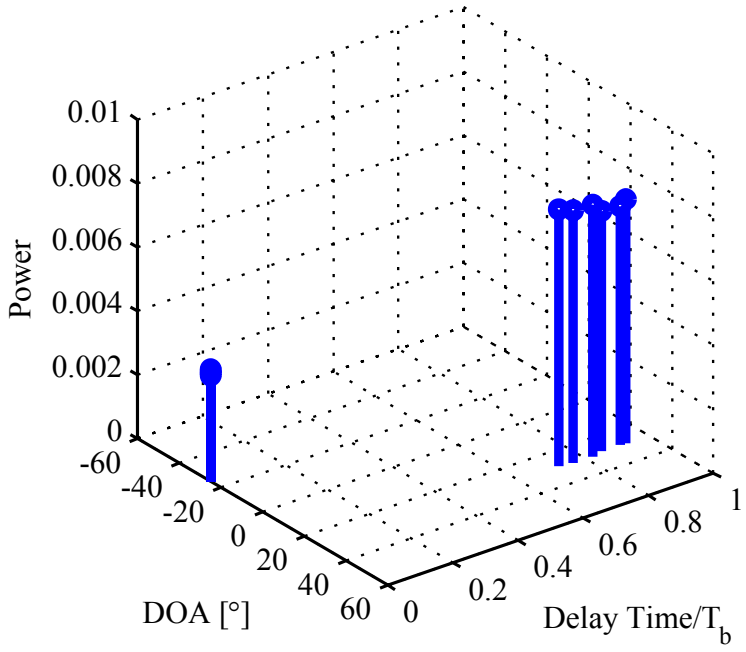

(b) Delay from 1 to 2 symbols (every 0.2 symbol)

Figure A.8: Estimation result of the proposed method (measurement).

(a) Experimental setup

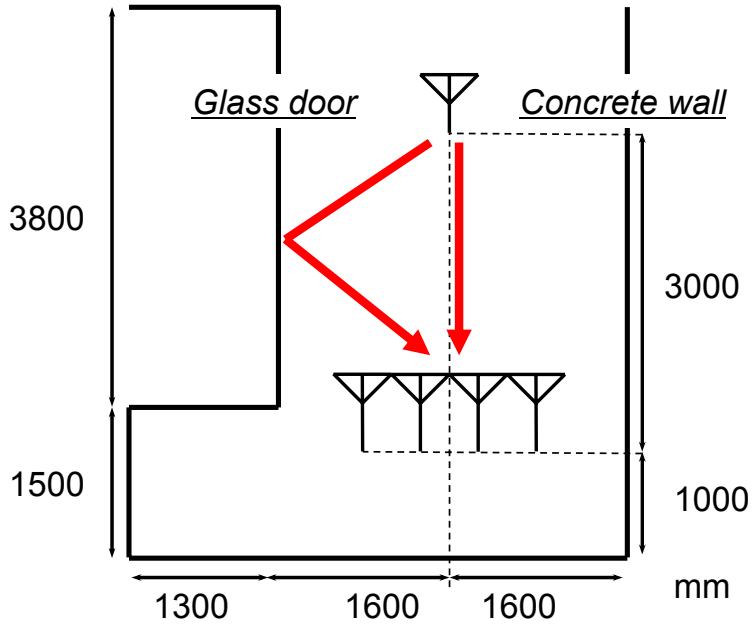

(b) Transmitting antenna and receiver array position

Figure A.9: Measurement in an indoor environment.

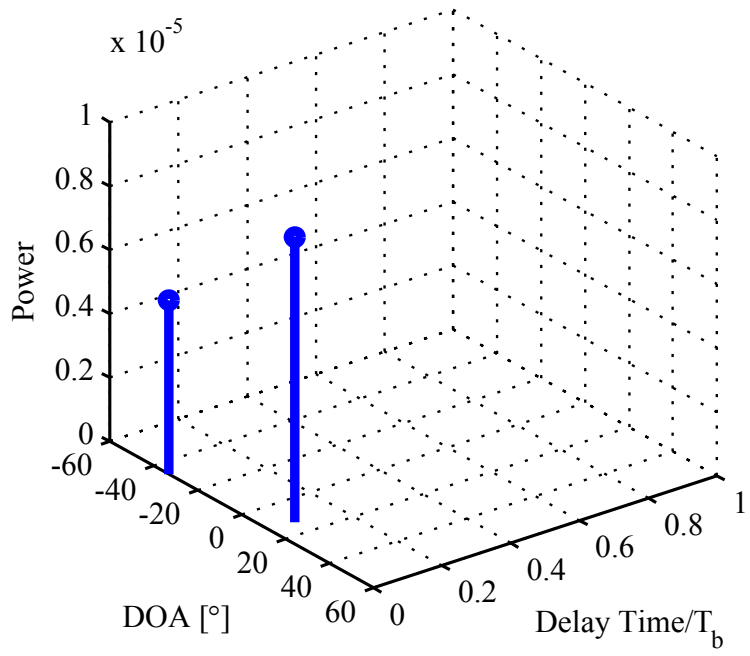

Figure A.10: Estimation result of the proposed method (measurement).

Table A.1: Experimental Specifications.

Modulation	QPSK
RF frequency	5 GHz
IF frequency	40 MHz
Base band signal	Random (repeat with 250 symbols)
Symbol rate	4 Msymbol/s
Sampling frequency	32 MHz (Undersampling)
Array antenna	0.5λ sleeve linear array
Snap shot	400 (50 symbols)

Acknowledgments

I wish to express my gratitude to my supervisor Professor Hiroyuki Arai to sincerely acknowledge his continuous guidance throughout this study. I am grateful to Professor Yasuo Kokubun, Professor Ryuji Kohno, Associate Professor Toshihiro Baba, and Associate Professor Koichi Ichige of the Yokohama National University for their helpful discussions and critical reading of the manuscript.

I am indebted to Dr. Yoshio Ebine, Dr. Keizo Cho of NTT DoCoMo, Inc., Dr. Koichi Tsunekawa of NTT Corporation, Masahiro Karikomi of Nihon Dengyo Kosaku Co. Ltd, and Mr. Kiyoshi Yamasaki of Adtex for their valuable suggestions and encouragement.

Thanks are also due to the members of Professor Arai's group at the Yokohama National University. I would like to acknowledge SCAT (Support Center Advanced Telecommunication) for the scholarship. Finally, I express my gratitude to my parents and family for their support.

Bibliography

[1] Hideichi Sasaoka, Mobile communication, Ohmsha, Ltd., Tokyo, 1998.

[2] N. Kikuma, Adaptive Signal Processing with Array Antenna, Science and Technology Publishing Co., Tokyo, 1999.

[3] B.Widrow, P.E.Mantey, L.J.Griffinths, and B.B.Goode, "Adaptive Antenna Systems," Proceedings of the IEEE, vol.55, No.12, pp2143-2159, Dec. 1967.

[4] H. Winters, "Smart Antennas for Wireless Systems," IEEE Pers. Commun., vol. 5, no. 1, pp. 23-27, Feb. 1998

[5] Yoshio Karasawa, Hideyuki Inomata, "Digital Beamforming Antennas in Communication Systems : As an Intelligent Antenna in the Future," The Journal of IEICE, Vol.78, No.9, pp.899-906, Sep.1995.

[6] Nobuo Nakajima, "Adaptive Array Antenna for Mobile Communications," Transactions of IEICE, Vol.J84-B, No.4, pp.666-679, Apr. 2001.

[7] Tomoyoshi Yokota, Kazuhiro Yamamoto, Jyunichi Jinno, Shigeru Kimura, Haruhito Kato, Masahiro Sada, "The Development of PHS Base Station with Adaptive Array Antenna," Proceedings of the Society Conference of IEICE, pp.324, 1998.

[8] R. T. Compton, Jr., Adaptive Antennas, Concepts and Performance, Prentice-Hall, 1988.

[9] J.R. Treichler and B.G. Agee, "A New Approach to Multipath Correction of Constant Modulus Signals," IEEE Trans. on ASSP, Vol. 31, No. 2, pp. 459–472, April 1983.

[10] Sidney P. Applebaum, "Adaptive Arrays," IEEE Trans. Antennas and Propagation, vol. AP-24, No.5, pp.585-598, Sept.1976.

[11] K. Takao, M. Fujita and T. Nishi, "An adaptive antennaarray under directional constraint," IEEE Trans. Antennas & Propag. vol.AP-24, No.5, pp.662-669, Sept.1976.

[12] RT Compton, Jr., “The power inversion adaptive array: Concept and performance,” IEEE Trans. Aerosp. Electron. Syst., vol. AES–15, pp. 803–814, Nov. 1979.

[13] R.O.Schmidt, “Multiple Emitter Location and Signal Parameter Estimation,” IEEE Trans. Antennas and Propagat., vol.34, no.3, pp.276-280, Mar. 1986.

[14] R.Roy, T.Kailath, “ESPRIT-Estimation of Signal Parameters via Rotational Invariance Techniques,” IEEE Trans., vol.ASSP-37, pp.984-995, July 1989.

[15] Steyskal and J.S.Herd, “Mutual coupling compensation in small array antennas,” IEEE Trans., vol.AP-38, no.12, pp.1971-1975, Dec. 1990.

[16] Akira Minakawa, Tadashi Matsumoto, “Effects of Steering Vector Distortion and its Compensation on DOA Estimation,” IEICE technical report. Antennas and propagation, AP2000-75, pp.1-6, Sep. 2000.

[17] Takahiro Arai, Hiroyoshi Yamada, Yoshio Yamaguchi, “On Calibration of Direction-of-Arrival Estimation with an Antenna Array,” IEICE technical report. Antennas and propagation, AP2000-133, pp.43-50, Oct. 2000.

[18] G.Tsoulos, J.McGeehan and M. Beach, “Space division multiple access (SDMA) filed trials Part2: Calibration and linearity issues,” IEE Proc. Radar, Sonar Nabig., col.145, No.1 pp.79-84, February 1998.

[19] R.T.Williams, S.Prasad, A.K.Mahalanabis, L.H.Sibul, “An improved spatial smoothing technique for bearing estimation in a multipath environment,” IEEE Trans., Acoustics, Speech, and Signal Processing, vol.36, pp.425-432, Apr.1988.

[20] Y.L.C.De Jong, M.H.A.J.Herben, “High-resolution angle-of-arrival measurement of the mobile radio channel,” IEEE Trans. Antenna and Propagat., vol.47, No.11, Nov. 1999.

[21] Y.Ogawa, N.Hamaguchi, K.Oshima, and K.Itoh, “High-resolution analysis of indoor multipath propagation structure”, IEICE, Trans. Commun., vol. E78B, pp.1450-1457, Nov. 1995.

[22] M.D.Zoltowski, M.Haardt, and C.P.Mathews, “Closed-Form 2-D Angle Estimation with Rectangular Arrays in Element Spase or Beamspase via Unitary ESPRIT,” IEEE Trans., Signal Processing, vol.44, No2, pp.316-328, Feb.1996.

[23] Y.Tanabe, Y.Ogawa, T.Ohgane, “High-resolution estimation of multipath propagation based on the 2D-MUSIC algorithm using time-domain signals,” IEICE Trans. Commnu., Vol.J-83-B, Apr. 2000.

[24] H.Nakahara, N.Kikuma, N.Inagaki, “Estimation of propagation delay time and direction of arrival indoor quasi-millimeter multipath waves using FFT-MUSIC with triangular antenna array,” Technical report of IEICE AP95-120, Feb. 1996, in Japanese.

[25] Y.Kuwahara, Y.Susukida, H.Kakinuma, S.Ogawa, “Development of Multipath Propagation Analysis Equipment,” IEICE Trans. J82-A No.6, pp.903-911, June 1999, in Japanese.

[26] T. Manabe and H. Takai, “Superresolution of multipath delay profiles measured by PN correlation method,” IEEE Trans. Antenna and Propagat., vol.40, pp.500-509, May 1992.

Publication List

The following list contains the publications cited in this dissertation.

Papers

1. Yuki Inoue, Hiroyuki Arai, "Effect of Mutual Coupling and Manufactural Error of Array for DOA Estimation of ESPRIT Algorithm," IEICE Trans Comm., Vol.J86-B, No.10, pp. 2145-2152, October 2003 (in Japanese).

2. Yuki Inoue, Hiroyuki Arai, "Pattern Calibration Free Antenna By Suppressing Mutual Coupling Between Elements," IEICE Trans.B (schedule).

3. Yuki Inoue, Kouji Shimizu, Hiroyuki Arai, "Signal Discrimination Method Based on the Estimation of Signal Correlation Using an Array Antenna," IEEE Trans., VTC (submitted).

International Conference

4. Yuki Inoue, Kohei Mori, Hiroyuki Arai, "DOA error estimation using 2.6GHz DBF array antenna," Asia-Pacific Microwave Conference, volume2, pp.701-704, Taipei, Taiwan, R.O.C., Dec.2001.

5. Yuki Inoue, Kohei Mori, Hiroyuki Arai, "DOA Estimation in consideration of the Array Element Pattern," IEEE Proceedings Vehicular Technology Conference Spring 2002, vol.2, pp.745-748, Birmingham, Al, May 2002.

6. Yuki Inoue, Kouji Shimizu, Hiroyuki Arai, Kazuhiro Komiya, Kouichi Tunekawa, "Signal Discrimination Method Based on the Estimation of Signal Correlation Using an Array Antenna," 2004 IEEE Vehicular Technology Conference, Milan, Italy, May 2004.

7. Yuki Inoue, Hiroyuki Arai, “Pattern Calibration Free Antenna By Suppressing Mutual Coupling Between Elements,” Proceedings of International Symposium on Antennas and Propagation, Sendai Japan, Aug 2004.

IEICE Technical Reports

8. Yuki Inoue, Kohei Mori, Hiroyuki Arai, “Study of DOA Estimation Error and Correction Methods using 2.6GHz and 8.45GHz Band DBF Array Antennas,” IEICE technical report. Antennas and propagation, Vol. 101, Num. 231, pp.19-24, July 2001 (in Japanese).

9. Yuki Inoue, Kouji Shimizu, Hiroyuki Arai, Kazuhiro Komiya, Kouichi Tunekawa, ” Discernment of Arrival Waves by the Estimation of Signal Correlation Matrix using an Array Antenna”, Vol. 103 Num. 63 pp.53-58, May. 2003 (in Japanese).

IEICE General Conference and Society Conference

10. Yuki Inoue, Kohei Mori, Hiroyuki Arai, Kazunori Watanabe, Ryuji Kohno, ”A model of standard propagation using low cost DBF receiver in a radio anechoic chamber,” Proceedings of the Society Conference of IEICE, B-1-27, pp.27, Sept. 2000 (in Japanese).

11. Yuki Inoue, Kohei Mori, Hiroyuki Arai, “Error of The DOA Estimation with A DBF Array Antenna,” Proceedings of the IEICE General Conference, B-1-44, pp.62, March 2001 (in Japanese).

12. Yuki Inoue, Kohei Mori, Hiroyuki Arai, “DOA Estimation Error and the Steering Vector of the DBF Array Antenna,” Proceedings of the Society Conference of IEICE, B-1-33, pp.39, Aug. 2001 (in Japanese).

13. Yuki Inoue, Kohei Mori, Hiroyuki Arai, “The Effect of Minute Change of a Linear Array Element Interval for DOA Estimation Error,” Proceedings of the IEICE General Conference, B-1-147, Mar. 2002 (in Japanese).

14. Yuki Inoue, Kohei Mori, Hiroyuki Arai, “The relation between Manufacturing Error of Array Element Position and DOA Estimation Error,” Proceedings of the Society Conference of IEICE,B-1-8, Jul.2002 (in Japanese).

15. Yuki Inoue, Kouji Shimizu, Hiroyuki Arai, Kazuhiro Komiya, Kouichi Tunekawa, ”The Measurement of DOA Estimation in Anechoic Chamber using 16 channels DBF Receiver,” Proceedings of the IEICE General Conference, B-1-117, Mar. 2003 (in Japanese).

16. Yuki Inoue, Kouji Shimizu, Hiroyuki Arai, Kazuhiro Komiya, Kouichi Tunekawa, ” Comparison of the Method in Discernment of Arrival wave using an Array Antenna,“ Proceedings of the Society Conference of IEICE, B-1-117, Jul.2003 (in Japanese).

17. Yuki Inoue, Hiroyuki Arai, “The measurement of Mutual Coupling Compensation of Transmitting Array in an Anechoic Chamber,” Proceedings of the IEICE General Conference, B-1-217, Mar. 2004 (in Japanese).

18. Yuki Inoue, Hiroyuki Arai, “5GHz Band 4×4 MIMO Prototype System and Measurement of Indoor Environment,” Proceedings of the Society Conference of IEICE, B-1-183, Sep.2004 (in Japanese).

Joint Work

Letters

19. Kohei Mori, Yuki Inoue, Koich Ichige. Hiroyuki Arai,”Experiments of DOA Estimation by DBF Array Antenna at 2.6GHz”, IEICE Trans. Comm., vol. E-84-B, No.7, pp1871-1875, July 2001.

International Conference

20. Kohei Mori, Yuki Inoue, Hiroyuki Arai, Kazunori Watanabe, Ryuji Kohno, ”The DOA Estimation using the Low Cost DBF Array Antenna”, ISAP2000, Vol.4, pp.1645-1648, Fukuoka, Japan, Aug 2000.

21. Kohei Mori, Yuki Inoue, Hiroyuki Arai, ”A digital beam forming by using low cost receiver at 2.6 GHz,” , ICAP2001, Manchester, UK. Apr 2001.

22. Kohei Mori, Yuki Inoue, Minseok Kim, Kouichi Ichige, Hiroyuki Arai, ”DBF array antenna systems at 8.45 GHz,”APS2001, Boston, U.S.A, Jul 2001.

23. Kouji Shimizu, Yuki Inoue and Hiroyuki Arai, “BER Measurement Using Beam Steering Adaptive Array Under Indoor Propagation Environment” Asia-Pacific Microwave Conference , New Delhi, India, Dec 2004.

IEICE Technical Reports

24. Naoto Ito, Yuki Inoue and Hiroyuki Arai, “Proposal of Array Calibration System using Multiple Sources and Study of Optimum Source Location”, IEICE technical report. Antennas and propagation, AP2004-19, May.2001 (in Japanese).

IEICE General Conference and Society Conference

25. Kohei Mori, Yuki Inoue, Hiroyuki Arai, Kazunori Watanabe, Ryuji Kohno, ” A DOA Estimation by using a low cost DBF receiver in an indoor environment”, Proceedings of the Society Conference of IEICE,B-1-26, Sep, 2000 (in Japanese).

26. Akimiti Hirota,Yuki Inoue, Kouichi Ichige, Hiroyuki Arai, “DOA and Electric Power Estimation Experiment by Adaptive Array Antenna”, Proceedings of the IEICE General Conference, B-1-20, Mar. 2002 (in Japanese).

27. Hirotake Sumi, Yuki Inoue, Hiroyuki Arai, “Error of The DOA Estimation for Two Incident Wave Case”, Proceedings of the Society Conference of IEICE, B-1-11, Sept. 2002 (in Japanese).

28. Hirotake Sumi, Yuki Inoue, Hiroyuki Arai, “Error of The DOA Estimation for Two Incident Waves”, Proceedings of the IEICE General Conference, B-1-115, Mar. 2003 (in Japanese).

29. Kouji Shimizu, Yuki Inoue, Hiroyuki Arai, “Estimation of DOA and Correlation Coefficient in Received Signal of Array Antenna”, Proceedings of the Society Conference of IEICE, B-1-118, Sept. 2003 (in Japanese).

30. Hirotake Sumi, Yuki Inoue, Hiroyuki Arai, “Patch Antenna Array with Metal Wall Box for Suppressing Mutual Coupling between Elements at 5GHz Band”, Proceedings of the IEICE General Conference, B-1-196, Mar. 2004 (in Japanese).

31. Kouji Shimizu, Yuki Inoue, Hiroyuki Arai, “An Indoor Experiment of BER Characteristics Based on DOA Estimation”, Proceedings of the IEICE General Conference, B-1-238, Mar. 2004 (in Japanese).

32. Kouji Shimizu, Yuki Inoue, Hiroyuki Arai, “Indoor Propagation Measurement of Beam Steering Array”, Proceedings of the Society Conference of IEICE, B-1-151, Sept. 2004 (in Japanese).

33. Naoto Ito, Yuki Inoue, Hiroyuki Arai, “An Experiment of Array Calibration System with Calibrating Antenna”, Proceedings of the Society Conference of IEICE, B-1-204, Sept. 2004 (in Japanese).